1-1-2014

Elastic Stability Of Flexural Members In Civil Engineering Design

Alexander Lamb
Wayne State University,

ELASTIC STABILITY OF FLEXURAL MEMBERS IN CIVIL ENGINEERING DESIGN

by

ALEXANDER W. LAMB

DISSERTATION

Submitted to the Graduate School

of Wayne State University,

Detroit, Michigan

in partial fulfillment of the requirements

for the degree of

DOCTOR OF PHILOSOPHY

2014

MAJOR: CIVIL ENGINEERING

Approved by:

_____

Advisor Date

_____

_____

_____

_____

DEDICATION

This work is dedicated to my mother and father who provided me with love and support unconditionally throughout my life.

And to my son, whenever you may be.

ACKNOWLEDGEMENTS

I would like to acknowledge my advisor Dr. Christopher Eamon for all of his guidance and effort on this dissertation and for his support throughout the process. I would also like to acknowledge my contemporary Kapil Patki for his efforts on the reliability portion of this dissertation.

I would also like to acknowledge my friends Dr. John Gruber and Dr. Dinesh Deveraj for all their time and mentorship over the years.

PREFACE

This work is prepared for compliance with the requirements of the degree of Doctor of Philosophy at Wayne State University. The research conducted and described in this dissertation document was conducted under the auspices of Dr. Christopher Eamon and the Department of Civil and Environmental Engineering at Wayne State University between September 2011 and September 2014.

This is an original work, except where acknowledgements and citations are provided. Neither this work nor any other work that is similar is being submitted for any other degree, certification or publication. This dissertation contains less than 20,000 words.

-Alexander Lamb

TABLE OF CONTENTS

LIST OF TABLES

LIST OF FIGURES

CHAPTER 1 INTRODUCTION

General

The elastic stability of flexural members has been an important consideration in civil engineering design since the beginning of the 20th century. With all buildings, bridges and the majority of the United States' critical infrastructure containing beams, the limit state of lateral torsional buckling continues to be prevalent even to this day. Bucking or instability is the propensity of a structural component or member to distort and deflect in directions that are not consistent with the direction of the applied loading. Elastic lateral torsional buckling of a flexural member is the instability associated with displacement of that member in both the lateral (with respect to the load) and torsional (with respect to the member) directions. This limit state is limited to the elastic material behavior region of the material being considered.

Buckling in flexural members may occur on both the local level and global level. On the local level, buckling occurs when the components that make up the larger structure or member begin to distort. This distortion is always in directions orthogonal to the direction of the stress in the component. Global buckling is the displacement on the member or structure level that occurs in directions that are orthogonal to the applied loading.

Design codes around the world have provisions for designing flexural members considering the limit state of lateral torsional buckling. The United States, Australia, Europe and Canada have advanced this limit in their design codes since their inception and continue to improve its characterization for practical designers to use. These

codices recognize that design engineers in ordinary circumstances do not have the resources to perform complex structural analyses for this limit state. As a result, efforts have been to produce shorthand methods that more or less adequately predict the strength of these members. These shorthand methods typically involve decoupling the effects that make up the lateral torsional buckling limit state and describing them using closed form factors. Although not all effects are as yet functionally described in prevailing design codes, the effects have been identified as: moment distribution between supports, effect of load height, restraint at member ends and along members' length, and buckling interaction.

Moment distribution between supports refers to the shape the moment function takes between support locations; brace points are not considered. The effect of load height refers to the vertical position of the load with respect to the shear center of the member. Restraint at member ends and along members' length refers to how the member is supported and what levels of bracing is applied. Buckling interaction is how buckling of the member is affected by adjoining structural elements.

Problem Statement

Flexural member design for the lateral torsional buckling limit state using the prevalent design codes of the United States, Australia, Europe and Canada consider the effect of moment distribution between supports and the effect of load height with respect to the shear center. All codices consider the effect of moment distribution between supports. Only the Canadian and Australian codes attempt to describe the load height effect. The effects of end restraint and buckling interaction are simply neglected

as they produce less of an effect on the stability of flexural members compared to moment distribution and load height.

To describe the effects of moment distribution between supports a closed form expression called the equivalent uniform moment factor is used. This factor (termed moment factor) is an attempt at modifying the basic strength of a loaded member by indexing its strength against the strength of a member loaded with a constant moment distribution. The factors used by these code works are inaccurate for some loading circumstances on both the conservative and unconservative ends of capacity prediction. This issue arises due to the broad range of moment distributions for which the factor is intended to predict capacities. Current efforts to improve the effectiveness of these moment factors involve producing expressions for specific loading types. Although extensive effort has been put into producing solutions for possible distributions, many loading scenarios remain uncharacterized. Without solutions for a comprehensive range of load distributions, it is unlikely design codes will alter their methods and use moment factors tailored to specific load distribution types.

The effects of load height are characterized in the design codes that consider this effect by modifying the members' effective length. This approximation is suggested in place of a more complex rational method. In the case of a load that serves to restrain the member against buckling from the load, the height of the loading is simply neglected for these codes that consider load height. When a member is loaded below its shear center the effective capacity of the member increases because the load acts to correct the torsional displacement tendency. When the load is above the shear center, however, the capacity decreases significantly as the load produces additional

destabilizing forces in the torsional direction. The design codes that neglect the effect of load height are in danger of producing structural components and therefor entire structures that are structurally deficient during critical phases of their life. The most significant of these phases being the construction period, as many of the members will be loaded in a standalone temporary fashion where they do not have suitable lateral bracing to ensure negation of the load height effect.

Objective and Scope of Research

The objective and scope of this research is to study the effects of moment distribution on the lateral torsional stability of flexural members for new and as yet uncharacterized load distribution types, and to produce load height factors for these distributions using a new method for decoupling load height and moment distribution effects using continuum mechanics derivation as substantive proof and to investigate the effect of moment distribution and load height on the reliability of steel members.

The moment distributions studied are those produced from an n^{th} degree spandrel load type with variable end moments. These spandrel load types can be converted into other continuous load types, such as a uniformly distributed load, uniformly increases load, and a parabolic nonlinear load. Moment factors are produced for these load types and compared with design codes to show the discrepancy that exists between their approximation and the true solution.

The load height effect is characterized by decoupling it from the effect of moment distribution and presenting it in terms of a load height factor. Load height factors are provided for these new load types studied and are intended to modify the basic strength

of a member in the same way the moment factors do. The moment factors and load height factors are intended to be used in conjunction while describing the lateral torsional buckling capacity of a member with the spandrel type loading. Either factor may be used exclusively without affecting the other to determine the change in capacity associated with each effect. Load heights are described from 0 inches to 22 inches which covers top flange loading of AISC 360 (AISC 2010) wide flange sections depths up to and including a W44.

Organization

This dissertation contains 8 chapters.

Chapter 1 provides an introduction to the instability problem associated with flexural members and describes the problem statement and objective and scope of the research.

Chapter 2 presents a state of the art review of the available literature sources that are used as the foundation for this work.

Chapter 3 provides derivation and general discussion on the mechanics used to model the instability issue.

Chapter 4 outlines the numerical method used to solve the governing differential equation relating to lateral torsional stiffness

Chapter 5 describes the mechanics used to develop the load height factors and presents them with practical design examples.

Chapter 6 presents some additional developments in elastic stability from the effect of various kinds of restraint.

Chapter 7 shows the results of a reliability analysis targeted to AISC 360 steel beams subject to loading above the shear center and moment distribution.

Chapter 8 presents the final conclusions drawn from the body of research presented heir in and the need for future research in the elastic stability area

CHAPTER 2 LITERATURE REVIEW

Introduction

Buckling or instability can be described as a sudden displacement or deformation in a direction not consistent with the direction of the applied load. That is to say that the displacement associated with instability is apparent in one or more of the axis orthogonal to the axis of the applied load. Lateral torsional buckling is instability associated with flexural members. The resulting instability from lateral torsional buckling is apparent in the direction orthogonal to the primary axis being loaded and directly, the member's torsional axis (Trahair 1993, Timoshenko and Gere 1961). This makes lateral torsional buckling a combination of destabilization of two of the six total primary planes of a member. The axis transverse to the length of the member and orthogonal to the plane of loading is referred to as the member's weak axis and the member's flexural stiffness in this direction resists destabilization in this direction. The torsional axis runs the length of the member and destabilization in this direction is resisted by the members torsional stiffness and warping stiffness. The warping stiffness of a cross section is the ability of the cross section to maintain its shape against distortion from an applied torsional load. Inherent to lateral torsional buckling for flexural members is that only members bent about their strong axis are capable of buckling this way (Nethercot and Trahair 1976). It is possible for these types of members to fail through torsional buckling; however, this failure mechanism is not the focus of this investigation (Clark and Hill 1960). Members that fail through lateral torsional buckling may be in two possible stress states at the onset of instability. These stress states are elastic and plastic for ductile materials such as steel. Elastic lateral torsional buckling is the result of

a member destabilizing while in the elastic stress range of the material. Inelastic lateral torsional buckling is the result of a member destabilizing while in a stress state beyond the elastic limit of the material. Typically, long thin flexural members are prone to elastic lateral torsional buckling while short stocky members are more susceptible to inelastic lateral torsional buckling, if buckling occurs at all (Kirby and Nethercot 1979).

Mechanisms Affecting Flexural Member Instability in Literature

Analytical computation of the lateral torsional stability of flexural members is practically impossible for all cases and exact solutions, in many cases, do not exist in the realm of current mathematics. Numerical solution methods are the resulting tools used to investigate these phenomena. It cannot be expected for the typical design engineer to employ these advanced methods to solve routine structural stability related limit state problems. Therefor it is necessary to develop alternative methods that produce accurate, conservative results that do not require significant computational effort. To develop these types of methods, a full review of relevant lateral torsional buckling literature is necessary. Review of relevant lateral torsional buckling literature shows four mechanisms that affect the elastic lateral torsional stability of flexural members (Nethercot and Trahair 1976, Wong and Driver 2010, Clark and Hill 1960):

1. Moment distribution between restraints
2. Varying levels of out of plane restraint at member ends and brace points
3. Load height with respect to shear center
4. Buckling interaction

Moment Distribution between Restraints

In most flexural member design scenarios, moment distributions between restraint locations are not uniform. These cases result in significant computational effort to solve bending stiffness equations, which is undesirable. To reduce computational effort, design codes almost exclusively use what is called the equivalent uniform moment factor approach (AISC 360 2010, Zuraski 1992). This method takes the analytical solution for the worst case scenario moment loading and assumes this to be the lowest possible destabilizing capacity for the member. Termed the basic strength, this worst case scenario corresponds to a simply supported beam, loaded with a constant moment distribution on its strong axis, at the members shear center (Kirby and Nethercot 1979). This is shown in Figure 1 and Figure 2.

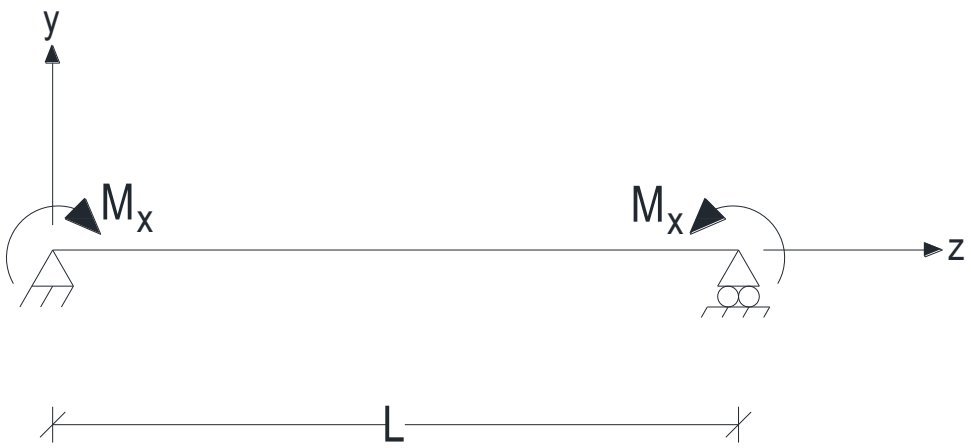

Figure 1: Simply supported beam, global view

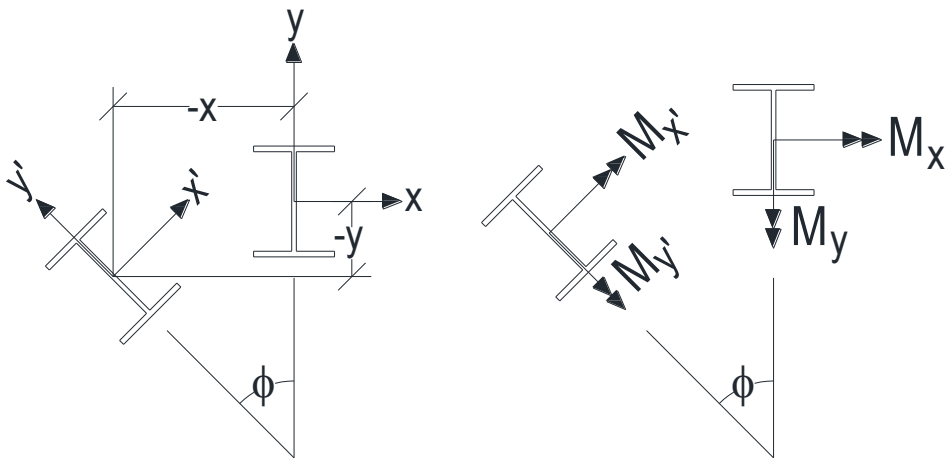

Figure 2: Simply supported beam, cross section view

To formulate a mathematical description of a flexural member that undergoes lateral torsional buckling affected by the described factors, the coordinate references shown in Figures 1 and 2 are used. Moment directions $M_{x'}$ and $M_{y'}$ correspond to a local coordinate system oriented on the buckled cross section, shown in Figure 2. Double arrows indicate moment directions following the right hand rule. The applied loads to the member are M_x, while other loads indicated are to show positive force directions only. Warping and twisting at the members ends, are assumed to be free and fully restrained respectively, with rotation about the members weak axis unrestrained. Bending stiffness equations for the beam are written about the local coordinates <x,y,ϕ>' as shown in Eq.'s 1, 2, and 3 respectively.

$$EI_x \frac{d^2y}{dz^2} = M_{x'} \tag{1}$$

$$EI_y \frac{d^2x}{dz^2} = M_{y'} \tag{2}$$

$$GJ\frac{d\phi}{dz} - EC_w\frac{d^3\phi}{dz^3} = M_{z'} \tag{3}$$

Eq.'s 1, 2, and 3 can be combined into one expression representing the twisting stiffness of the member as shown in Eq. 4 using directional cosine information between local and global coordinates (Trahair 1993, Timoshenko and Gere 1961).

$$\frac{d^4\phi}{dz^4} - \frac{GJ}{EC_w}\frac{d^2\phi}{dz^2} - \frac{M_x^2}{E^2I_yC_w}\phi = 0 \tag{4}$$

The variable parameters used in the elastic lateral torsional buckling analysis for doubly symmetric members shown, more formally, are the member's weak axis moment of inertia, I_y, and the member's torsional parameter which contains warping and torsion stiffness relations. The torsion parameter is expressed in Eq. 5 as:

$$\frac{\pi}{L}\left(\frac{EC_w}{GJ}\right) \tag{5}$$

Where E is the materials modulus of elasticity, C_w is the cross sections warping constant, G is the materials shear modulus, J is the torsional inertia of the cross section, and L is the lateral and torsional unbraced length of the member. Eq. 5 can be seen in the equation for the basic lateral torsional buckling strength, Eq. 6. Eq. 6 is the analytically exact solution for M_x in Eq. 4, corresponding to a simply supported member loaded with a constant moment distribution (Trahair 1993, Timoshenko and Gere 1961).

$$M_{x,cr} = \frac{\pi}{L}\sqrt{EI_yGJ\left(1+\frac{EC_w}{GJ}\frac{\pi^2}{L^2}\right)} \tag{6}$$

With the basic strength shown in Eq. 6, numerical solutions are developed for other moment distributions and indexed against the basic strength so as to produce an equivalent uniform moment factor. This equivalent uniform moment factor multiplied by the basic strength for a member produces an approximate solution to the lateral torsional stability that flexural member with accuracy dependent on the method used. To eliminate the need for numerical analysis and thus increase computational efficiency, the equivalent uniform moment factor using the basic strength approach is employed. For these types of systems as they pertain to routine design, two methods are employed. These methods employed, capture the relative trends in the rates of change of various moment distributions between braces both generally and discretely. That is to say, some expressions cover all possible types of moment distribution between braces with one closed form expression, while others cover specific moment distributions individually (Serna et al. 2006, Lopex et al. 2006). In general, the methods that cover general types of moment distributions are less accurate when compared against numerically convergent solutions than those that are tailored to specific distributions of moment directly (Suryoatmono and Ho 2002, Wong and Driver 2010)]. The work done in these areas can be classified as follows:

a. Methods developed for unequal end moments (Austin 1961, Salvadori 1955)

b. Methods developed for general moment distributions (Serna et al. 2006, Kirby and Nethercot 1979)

c. Methods developed for specific moment distributions (Trahair 1993, Suryoatmono and Ho 2002, Clark and Hill 1960)

a. Methods developed for unequal end moments

The first attempts at describing the impact of moment distribution on later torsional buckling of flexural members produced results that are capable of handling cases where the rate of change of the moment functions are constant, that is to say the moment functions are uniform or linear only. More specifically, they are capable of handling cases that have applied end moments as the only applied forces causing bending. These relations are shown in Eq. 7 (Salvadori 1955) and Eq. 8 (Austin 1961).

$$C_b = 1.75 + 1.05\kappa + 0.3\kappa^2 \leq 2.3 \quad (7)$$

$$C_b = (0.6 - 0.4\kappa)^{0.1} \leq 2.5 \quad (8)$$

C_b represents the equivalent uniform moment factor (often referred to as the moment gradient factor) and κ is a parameter that quantifies the bending induced flange compression force variation along the length of the unbraced segment (Zuraski 1992). These show that members having variation that result in both compression and tension within the unbraced segment are less susceptible to destabilization than those under compression through the entire length. Eq. 7 represents a lower bounded solution using the Rayleigh-Ritz method while Eq. 8 comes from analysis work done on beam-columns. The limitation to these equations is obvious. Very few practical cases have flexural members loaded with only end moments.

b. Methods developed for general moment distributions

Due to the limitations of Eq.'s 7 and 8, expressions for general moment distributions are available as shown in Eq. 9 (Serna et al. 2006) and Eq. 10 (Kirby and Nethercot 1979).

$$C_b = \sqrt{\frac{35M_{max}^2}{M_{max}^2 + 9M_a^2 + 16M_b^2 + 9M_c^2}} \tag{9}$$

$$C_b = \frac{12M_{max}}{2M_{max} + 3M_a + 4M_b + 3M_c} \tag{10}$$

In these equations, M_{max} is the absolute value of the maximum moment with an unbraced segment, M_a is the absolute value of the moment at 25% of the unbraced segment, M_b is the absolute value of the moment at 50% of the unbraced segment, and M_c is the absolute value of the moment at 75% of the unbraced segment. Although in these papers it does not indicate to use the absolute value of these moments, it is generally recognized that this is to be true (AISC 360 2010, Wong and Driver 2010). Eq. 9 is the simplified result of curve fitting the data of numerical analysis that focused on the gradient of moment and the various level of lateral, torsional, and warping restraint at support locations. This section deals specifically with the effect of moment distribution between support locations, therefore Equation 9 represents a simplified version that considers free lateral restraint, and fixed torsional and warping restraint at supports. Eq. 10 is developed to allow for calculation independence of the magnitude of the end moments, unless one or both are the maximum moment within the unbraced segment under consideration. Additionally, Eq. 10 is developed to provide a way to describe the

degree of non-uniformity and its effect on flexural member stability. The issue with these general expressions for moment factor is their lack of accuracy in predicting capacity based on lateral torsional buckling. in some cases these expressions produce unconservative results. Some circumstances where unconservative results are produced are when there are abrupt changes in the distribution of moment, as is the case when members are loaded with concentrated moments along their unbraced length. Cases of reverse curvature bending also cause inherent problems with these closed form type expressions. Some preliminarily work has been done to show a divergence in these solution types as member length changes (Serna et al. 2006).

c. Methods developed for specific moment distributions

Instead of the general approach taken above, methods are available that consider specific moment distributions and have results tailored specifically to each type. A total of 12 moment distributions are studied and presented in the available technical literature. These moment distributions are covered by (Trahair 1993, Clark and Hill 1960, Suryoatmono and Ho 2002). The 12 moment distribution types are shown below in Table 1.

Distribution Type	Loading and Support Conditions
1	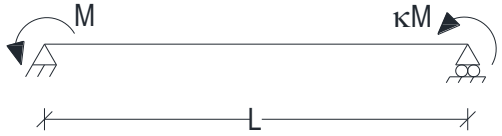

2	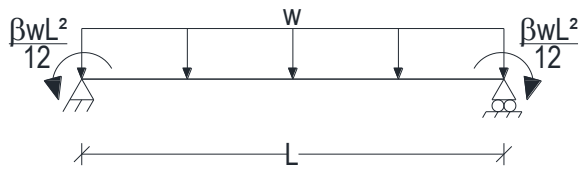
3	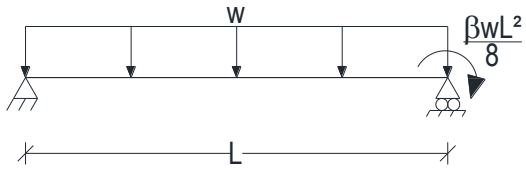
4	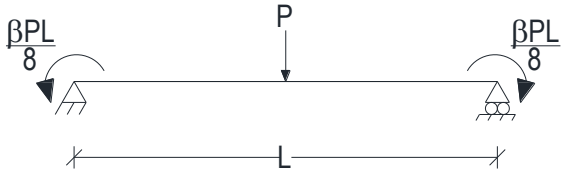
5	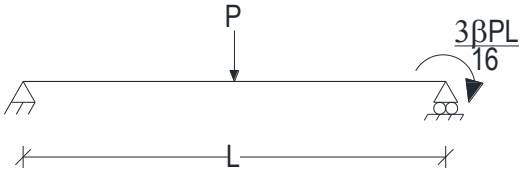
6	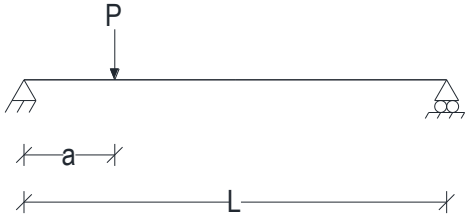
7	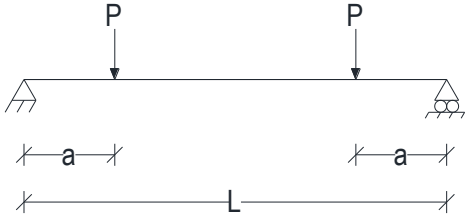

8	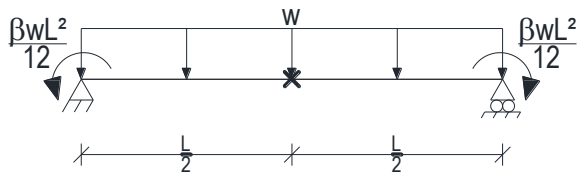
9	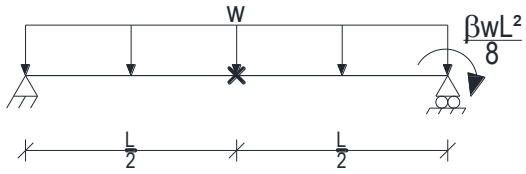
10	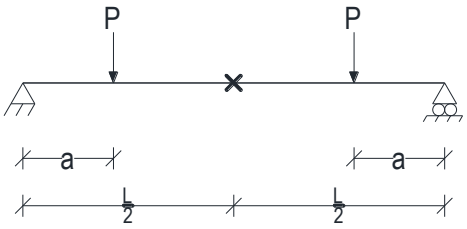
11	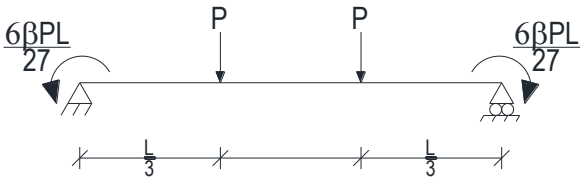
12	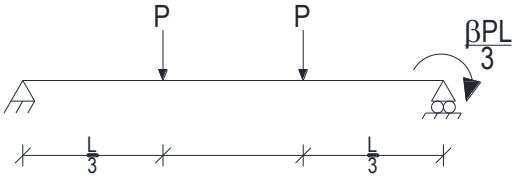

Table 1: Moment distribution types studied in literature

Contained within Table 1 are common load and dimension variables. The load variables are represented by *P*, *M* and *w* which represent concentrated loads, applied moments, and distributed loads respectively. Dimension variables are represented by *L* and *a*. In addition to these common variables are more complex factors κ and β. Factor

κ represents the ratio of the absolute value of the smaller to larger end moments. Factor κ is considered as positive for double curvature bending and negative for single curvature bending. These end moments for this factor are taken from within each unbraced segment. β represents the ratio of the applied end moment to the fixed end moment. Moment types 8, 9, and 10 have a lateral and torsional brace at the midspan and are otherwise simply supported. All other moment types are unbraced along their span lengths and are simply supported at the member ends. While these 12 cases do not provide a comprehensive set of solutions for all possible design scenarios, they are thought to provide a substantial enough reference point for moment factors relating to typical design (Trahair 1993, Clark and Hill 1960). Some important load cases are missing from the literature and they are uniform loading (triangular) and parabolic or nonlinear load types.

An inherent drawback to this type of moment factor classification is the wide variety of brace dimensions required for typical design. Braces are likely to occur in many different placed along the members length, the middle is just one possible location. Often, brace locations are not determined by the engineer, but architects and others responsible for facilitation of the overall structures aesthetics and functionability. A wider range of brace location possibilities for this type of method are required to cover more typical design cases.

Varying Levels of Out of Plane Restraint

The second factor affecting the lateral torsional stability of flexural members addresses the effects of torsional, lateral and warping end restraint in the out of plane

directions. Some work is done in the literature to characterize free and fixed end conditions in the out of plane directions, but no trend information is presented to accommodate intermediate values of restraint. Further, these sources consider only the effects of lateral bending restraint and warping restraint, torsional restraint is not considered (Serna et al. 2006, Lopex et al. 2006, Austin et al. 1955). The boundary conditions associated with these types of end restraint are represented in Expressions 11, 12 and 13, respectively. These expressions are shown as being set to zero, but they may be changed otherwise to represent other restraint types.

$$\frac{d^2x}{dz^2} = 0, \quad \text{at} \quad z = \begin{Bmatrix} 0 \\ L \end{Bmatrix} \tag{11}$$

$$\frac{d^2\phi}{dz^2} = 0, \quad \text{at} \quad z = \begin{Bmatrix} 0 \\ L \end{Bmatrix} \tag{12}$$

$$\phi = 0, \quad \text{at} \quad z = \begin{Bmatrix} 0 \\ L \end{Bmatrix} \tag{13}$$

Expressions 11 and 12 represent unrestrained lateral bending and warping end conditions, while Expression 13 represents fully fixed end conditions for twisting type deformation about the z-axis. Literature sources use factors k_1 and k_2, which are similar to column effective length factors (AISC 360 2010), to handle end conditions associated with Expressions 11 and 12. For a free lateral bending restraint end condition and a free warping restraint end condition k_1 is equal to k_2, which is equal to 1.0. For fully fixed lateral bending and warping end restraint k_1 is equal to k_2, which is equal to 0.5 (Serna et al. 2006, Lopez et al. 2006). To better describe the end restraint factors as analogous

to column effective length factors, a simple graphical approach is described using Figure 3 and 4.

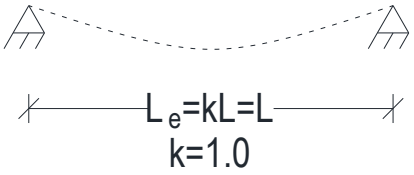

Figure 3: First buckled shape for simply supported member

Figure 3 shows a simply supported member and the relative buckled shape. If this shape is considered as the first buckled shape corresponding to *k* values of 1.0, it can be compared against the buckled shapes of other restraint cases to try and find the number of occurrences within a unit unbraced length being considered. The ratio of these occurrences is essentially the effective length for a particular support condition. This is graphically analogous to indexing the mathematical solution for a specific restraint condition to the base simply supported case.

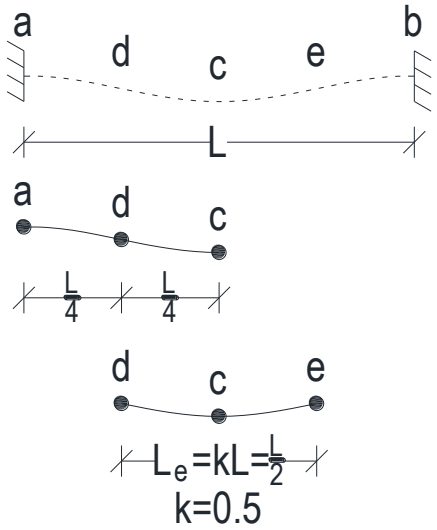

Figure 4: First buckled shape for a fully fixed member

Figure 4 shows directly the implementation of the effective length factor. For the fully fixed member shown, it can be identified that locations d and e are inflection points and therefore beam segment dce represents the basic buckled shape shown in Figure 3. Beam segments ad and eb when superimposed at points *a* and *b*, also form the basic buckled shape in Figure 3. Totaling the number of times this basic shape appears reveals 2 total occurrences making the effective length of this equal to 0.5. For other end conditions such as those that are unsymmetrical and those that are not idealized (pin, fix, free), it can be difficult if not impossible to use this graphical method to determine effective length factors as it relies heavily on symmetry and geometrically identifiable mathematical relationships such as inflection points and locations of zero rotation. For cases such as these, the problem must be formulated mathematically. The formulation can be as simple as performing a numerical analysis for a member with determinant end conditions and indexing these against the results of an analysis considering this same member as simply supported.

Load Height With Respect to Shear Center

The resistance of flexural members against lateral torsional instability can be affected significantly by the location of applied loads vertically relative to a cross sections shear center. A conclusion drawn previously in this work is that members bent about their weak axis are not capable of lateral torsional instability. It can be shown that members bent about their weak axis where $I_x \geq I_y$ will destabilize laterally under appropriate circumstances where the load is applied above the shear center of the cross section [6]. Further, under certain circumstances members will undergo a form of pure torsional destabilization.

To develop an analytical approach to assess the effect of load height, a free body diagram is composed with a load *P* acting some height y_v away from a cross sections shear center, shown in Figure 5.

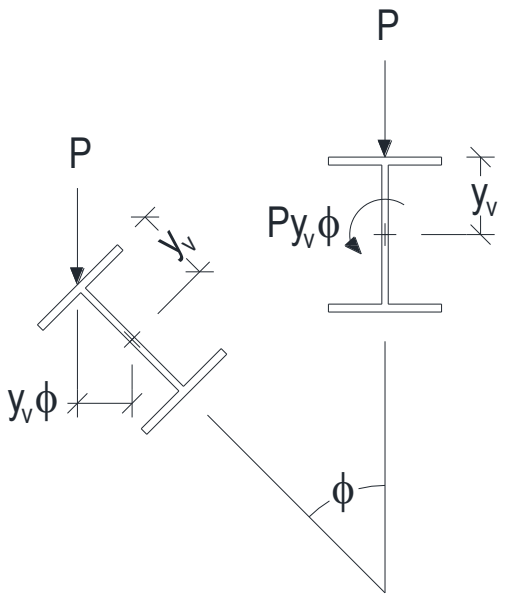

Figure 5: Free body diagram, load height analysis

This case considering a variable concentrated load is used for initial explanation because of its simplicity. Figure 5 shows the displaced cross section as a result of lateral torsional instability. As the cross section undergoes twisting type deformation (ϕ) additional torsion is imposed as a result of the applied transverse loads offset from the cross sections shear center (y_v) caused by the differential rotational displacement along the beam length. The additional torsional load imposed is equal to the rotation angle multiplied by the distance from the load to shear center (in the plane of the load) and multiplied by the magnitude of the load. This can be seen mathematically in Expression 14 and graphically in Figure 5.

$$M_{z,p} = Py_v\phi \quad (14)$$

Here, $M_{z,p}$ is the additional torsional load that is imposed. In terms of the torsional stiffness equation presented in Eq. 3, $M_{z,p}$ is considered as negative for cases where the load is applied below the cross sections shear center. This will result in an increase in the member's lateral torsional stability. Consider applying the load P in Figure 5 to the bottom flange of the member cross section shown. It is apparent that doing so will produce helping rotation to restore the member to its stable position. For cases with loads above the cross sections shear center, $M_{z,p}$ is considered as positive.

Work in this area is limited in scope and as a result practical solutions for designs are not well developed. Australian and Canadian design codes use an effective length factor approach where the beam length is considered as slightly longer to modify the basic strength for the equivalent uniform moment factor approach presented previously (CSA 2001, SAA 1998). This approach is for circumstances where the beams are not restrained by the loads causing the buckling and where lateral bracing at the top flange is not otherwise provided. Methods to handle concentrated loads and distributed loads above the shear center are available for specific locations respective to the shear center of the member only. That is to say for global member analysis simplified methods do not exist without performing higher level numerical methods. Some work is needed in this area to address this effect for some common load cases. The common load cases discussed in Table 1 would benefit from the study of this effect. A general trend as load height changes would be beneficial along with some kind of load height factor to be used in ordinary design circumstances that will provide an approximate solution.

Buckling Interaction

Buckling interaction deals specifically with the ability of unbraced adjacent unbuckled elements to restrain buckling of a more critical section. A simple example of this is a two span simply supported continuous beam, with unsymmetrical loadings relative to each span. When one span becomes unstable, assuming the beam deflection remains smooth and continuous, an inflection point will form and at this location buckling resistance is negligible. This is shown in Figure 6 with the dashed line representing an overhead view of the three dimensional buckled shape.

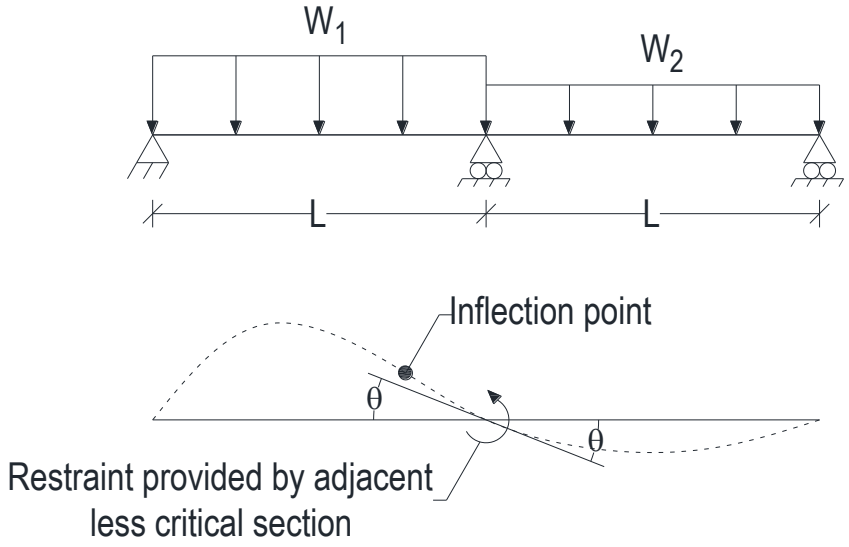

Figure 6: Buckling interaction for 2 span simply supported continuous beam

Essentially the unbraced segment that does not buckle (the right span) provides elastic restrain to the segment that does buckle (the left span). Based on the type and geometry of the structure a set of cases can be developed to describe the different types of buckling interaction cases apparent in this two span continuous system. For the symmetric structure shown in Figure 6 there are 3 possible cases considering the two

discrete load types W_1 and W_2 shown. These cases (a, b, and c) can be seen in Figure 7.

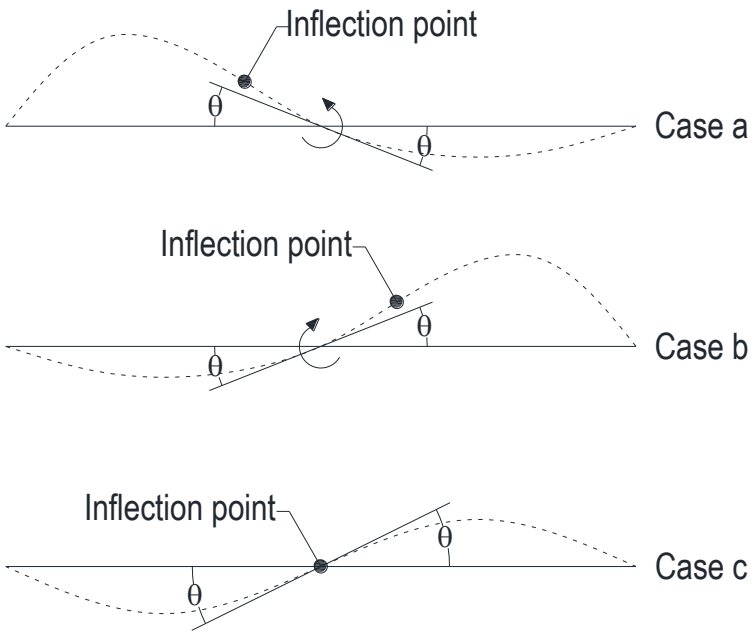

Figure 7: Buckling interaction cases a, b and c

Case a for this structure is shown in Figure 7. This case represents a scenario when $W_1 > W_2$ and an inflection point forms within the buckled span (left span). Case b occurs when $W_1 < W_2$ and an inflection point forms in the right span. In these two cases, it is assumed that the span containing the larger load dominates the overall structures buckling. Cases a and b are antitheses of one another. Case 3 corresponds to a scenario when $W_1 = W_2$ and the inflection point forms at the middle support. For this case the two unbraced segments are considered to buckle equally and because the inflection point forms at the support for this case, the effect of buckling interaction is not apparent. Buckling interaction is caused by the influence of other adjacent members providing some degree of variable restraint at locations of the members' intersection.

Because of this, the breadth of coverage in literature sources is minimal with a need for additional research with regards to specific system characterization.

In general current code works do not consider the effects of load height, end restraint, and buckling interaction. Excluding the effects of buckling interaction is acceptable because it will improve the resistance of flexural members against lateral torsional instability. The effects of load height and end restraint should not be excluded because unconservative results are possible in many circumstances. End restraint and load height in fact can produce the most severe effects as their influence can change the governing flexural limit state that causes a member to fail. Discussed above are the two limits that may be produced from this effect as induced lateral torsional buckling of weak axis bent member where $I_x > I_y$, and the propagation of the limit state of pure torsional buckling.

Relevant Code Procedure

To understand the current state of the practice in handling the elastic stability of flexural members, several design specifications and code manuals are reviewed. The specific codes and specifications studied are:

1. Specification for Structural Steel Buildings (AISC 360 2010)
2. LRFD Bridge Design Specifications (AASHTO 2012)
3. Structural Use of Steelwork in Building: Code of Practice for Design – Rolled and Welded Sections (BSI 2000)
4. Australian Standard: Steel Structures, (SAA 1998)

5. Limit States Design of Steel Structures, (CSA 2001)

6. Canadian Highway Bridge Design Code, (CSA 2006)

7. Design of Steel Structures, (ECS 1992)

These code works and specifications present a comprehensive review of the current relevant standards used throughout the international construction and design community. Contained within this list are two American specifications, two Canadian specifications, two European specifications and one Australian specification. All works use the equivalent uniform moment factor approach to handle the moment distribution between supports.

1. AISC 360-10, Specifications for Structural Steel Buildings

The American steel works specification considers only the distribution of moment between supports as having an effect on flexural member stability. A quarter points moment method is used here as described for Eq.'s 9 and 10. The expression for moment factor is shown in Eq. 14.

$$C_b = \frac{12.5M_{max}}{2.5M_{max} + 3M_a + 4M_b + 3M_c} \leq 3.0 \qquad (14)$$

The difference between Eq.'s 10 and 14 is the coefficient applied to the segments maximum moment, M_{max}. This coefficient has been adjusted to more adequately fit scenarios with fixed member ends (AISC 2010). Eq. 14 is applicable to all moment distributions with the exception of cantilever members where the free end is unbraced. In this such case, the moment factor C_b = 1.0. For all other applicable cases,

the moment factor is limited to 3.0. This value of 3.0 is the largest allowance for this type of factor amongst any of the design specifications considered (AISC 360 2010). This general closed form factor which is intended for use with any moment distribution is in many cases inaccurate.

2. AASHTO, LRFD Bridge Design Specifications

Similar to the American steel works specification, the AASHTO bridge code considers only the effects of moment gradient on flexural member stability. The expression for equivalent moment factor is the same as AISC 360 and also allows for the consideration of the expression shown in Equation 7 (presented differently however) under the appropriate circumstances. The form of this expression used by AASHTO is shown in Eq. 15.

$$C_b = 1.75 + 1.05\left(\frac{f_1}{f_2}\right) + 0.3\left(\frac{f_1}{f_2}\right)^2 \leq 2.3 \qquad (15)$$

Variable f_1 is the stress without consideration of lateral bending at the brace point opposite to the one corresponding to f_2. The variable f_2 is the largest compressive stress without consideration of lateral bending at either end of the unbraced length of the flange under consideration. Further, Eq. 15 is limited to C_b = 1.0 for cantilevers with the free end unbraced, for members where $f_{mid}/f_2 > 1$ or $f_2 = 0$, and for situations when the larger end moment is not the largest moment within the unbraced segment under consideration. The variable f_{mid} is the stress without consideration of lateral bending at the middle of the unbraced length of the flange under consideration. This equation is

applicable to members loaded with only end moments therefor moment diagrams must be transformed to accommodate this requirement (AASHTO 2012).

3. BS 5950-1, Structural Use of Steelwork in Building: Code of Practice for Design

The British specification considers the effects of moment gradient between supports using the same approach as shown in Eq. 14, however, the upper limit is lower and different weights are applied to the mid span moments. The moment factor used is shown in Equation 16. This specification has the lowest upper limit of any of the code works studied (BSI 2000).

$$C_b = \frac{M_{max}}{0.2M_{max} + 0.15M_a + 0.5M_b + 0.15M_c} \leq 2.273 \qquad (16)$$

4. AS 4100, Australian Standard: Steel Structures

The Australian specification considers the effects of moment gradient between supports, the type of support at unbraced segment ends, and the height of the load with respect to the shear center. The moment factor used employs a square root format and is shown in Eq. 17.

$$C_b = \frac{1.7M_{max}}{\sqrt{M_a^2 + M_b^2 + M_c^2}} \leq 2.5 \qquad (17)$$

The effects of end restraint and load height are addressed through the use of factors to be applied directly to change the unbraced length to an equivalent unbraced length. L_e, the equivalent unbraced length, is the unbraced length multiplied by factors k_t, k_l and k_r. These factors represent the twist restraint factor, the load height factor and

the lateral rotation restraint factor respectively. This effective length, L_e, is used in the basic strength equation shown previous in Eq. 6. To determine these k factors, SAA refers designers to the use of some code works published design tables (SAA 1998).

5. CSA-S16-01, Limit States Design of Steel Structures

The Canadian design specification uses an equivalent uniform moment factor approach to handle moment gradient between support locations. The equation used is the same as shown in Eq. 7, however, with an upper limit of 2.5 instead of 2.3. This is shown in Eq. 18.

$$C_b = 1.75 + 1.05\kappa + 0.3\kappa^2 \leq 2.5 \quad (18)$$

No indication is provided as to whether expression applies to transverse loads. The typical assumption with this expression is that it is for end moments and distributions that are linear. Additionally, this specification requires that C_b = 1.0 for any circumstance where there exists a moment within an unbraced segment that is larger than either end moment, effectively negating the beneficial effect entirely (CSA 2001). Load height is also addressed in the form of an effective length modification factor.

6. CSA-S6-06, Canadian Highway Bridge Design Code

The Canadian equivalent to the United States AASHTO bridge code, this specification has adopted the methods required in CSA 2001. In addition to the methods described in CSA 2001, some alternative methods are described. These methods correspond directly to those published by Clark and Hill for moment Types 1 through 12 shown in Table 1 (Clark and Hill 1960, CSA 2006).

7. Eurocode 3 EN-1993-1-1, Design of Steel Structures

The European design code is adopted in part of whole by many countries and is among the most popular codes in amongst the international community. To handle the stability of flexural members, Eurocode uses an equivalent moment factor approach and refers users to lateral torsional buckling curves along with table values for specific moment distributions. The moment distributions described correspond directly to Types 1, 2, 4 and 7 shown in Table 1 (ECS 1992).

Testing and Experimental Studies

To verify the aforementioned mechanisms' effects on lateral torsional stability of flexural members has been quantified accurately, or at least conservatively, experimental data are needed. These data are required to prove each effect individually and superimposed onto one another. These data are also required to prove elastic buckling theory for the system being studied. Elastic buckling theory must be verified through testing so the limits to these mechanisms effecting stability defined analytically are proven experimentally. An example of this is the boundary at which a member fails while in an elastic stress range or plastic stress range for the material, assuming buckling occurs as opposed to yielding or fracture of some type prior to these other failure mechanisms propagating. Because these other failure mechanisms are possible, clearly defining the boundaries between them (in terms of stress or force) is critically important to the proper implementations of limit state design procedures.

Elastic lateral torsional buckling has been verified for a few load cases and cross section types. Testing has primarily been done on sections made of aluminum. The test

cases include: tests on thin walled structures in general (Wang et al. 2012), symmetrical I-beams under uniform moment (Dumont and Hill 1940), unequal end moments (Clark and Jombock 1957), concentrated load at center span (Flint 1950), and rectangular cross sections (Dumont 1937), channels and z-shapes (Hill 1954). These tested cases prove elastic lateral torsional buckling theory for each of the cross sections studied. They also provide a good description of the limits of specific members for elastic lateral torsional buckling.

A study performed by Wang, Yuan, Shi and Cheng describes an experimental setup for fixed end restrained aluminum I-beams (Wang et al. 2012). The beams are provided by a manufacturer and material properties are verified by cutting sections from flanges and webs. The dimensions of each specimen are recorded along with other material properties tested such as modulus of elasticity and yield stress. The test setup uses bolted angles to provide fixity at the members ends. The members are loaded with 2 symmetric concentrated loads.

CHAPTER 3 ELASTIC STABILITY MECHANICS

General

The lateral torsional buckling stiffness is formulated using differential equations to allow for the solution to be tailored to the effects of moment distribution and load height. These differential equations are based on the work of Timoshenko and Gere (1961) and Trahair (1998) with some modifications. These differential equations are formulated according to the cross section undergoing lateral torsional displacement shown in Figure 2. Force equilibrium is used as the method for constructing the differential equation from the differential stiffness in the primary rotational directions.

Basic Strength

The basic strength is the elastic lateral torsional buckling capacity of a member loaded with a constant moment distribution. To determine the basic strength, rotational equilibrium is taken about the *x*, *y*, and *z* axes as defined in Figure 1. The rotational equilibrium equations about these axes are shown in Eq.'s 1, 2, and 3. Combining these equations and using the directional cosine information found in Table 2 to transform between the displaced and undisplaced cross sections ($m_{x'} = m_x$, $m_{y'} = \phi m_x$, and $m_{z'} = -\frac{dx}{dz} m_x$), yielding Eq. 19.

Coordinates	x	y	z
x'	1	ϕ	$-\frac{dx}{dz}$
y'	$-\phi$	1	$-\frac{dy}{dz}$
z'	$\frac{dx}{dz}$	$\frac{dy}{dz}$	1

Table 2: Directional cosines between buckled and unbuckled cross sections

$$GJ\frac{d\phi}{dz} - EC_w\frac{d^3\phi}{dz^3} = -\frac{dx}{dz}m_x \tag{19}$$

By putting Eq. 19 into standard form, as shown in Eq. 4, the differential equation may be solved for analytically using standard methods as outlined in Nagle et al. 2004. The general solution to the differential equation shown in Eq. 4 and the auxiliary solution are provided in Eq. 20 and Eq. 21 respectively.

$$\phi(z) = c_1\sin(gz) + c_2\cos(gz) + c_3e^{kz} + c_4e^{-kz} \tag{20}$$

$$r^4 - Ar^2 - B = 0 \tag{21}$$

Where,

$$A = \frac{GJ}{EC_w} \tag{22}$$

$$B = \frac{M_x^2}{E^2I_yC_w} \tag{23}$$

$$r^4 - Ar^2 - B = 0 \tag{24}$$

$$< k,g >^2 = \frac{A \pm \sqrt{A^2 + 4B}}{2} =< r_1, r_2 >^2 \tag{25}$$

The boundary conditions imposed on this system correspond to a simply supported beam with torsion fixed and warping unrestrained at the member ends. The relations for these boundary conditions are shown in Eq.'s 26 and 27 respectively.

$$\phi = 0, \quad \text{at} \quad z = \begin{Bmatrix} 0 \\ L \end{Bmatrix} \tag{26}$$

$$\frac{d^2\phi}{dz^2} = 0, \quad \text{at} \quad z = \begin{Bmatrix} 0 \\ L \end{Bmatrix} \tag{27}$$

Once these boundary conditions are imposed, the general solution may be differentiated and solved at these values. The resulting expressions allow a system of equations to be used to solve for constants c_1, c_2, c_3, and c_4. The expressions are as follows:

$$\phi(0) = c_2 + c_3 + c_4 = 0 \tag{28}$$

$$\phi(L) = c_1 \sin(gL) + 2c_4 \sinh(kL) = 0 \tag{29}$$

$$\frac{d^2\phi(0)}{dz^2} = -g^2 c_2 + k^2 c_3 + k^2 c_4 = 0 \tag{30}$$

$$\frac{d^2\phi(L)}{dz^2} = -g^2 c_1 \sin(gL) - 2k^2 c_4 \sinh(kL) = 0 \tag{31}$$

Solving for the constants yields the equation for twist as shown in Eq. 32. Once these constants are determined, Eq. 20 is used along with the auxiliary equation shown in Eq. 21 and its solution form shown in Eq. 25 to obtain the expression for critical moment.

$$\phi(z) = c_1 \sin(gz), \quad \text{at} \quad z = \begin{Bmatrix} 0 \\ L \end{Bmatrix}, \quad \phi = 0 \tag{32}$$

Solving for *g* shows that the first buckled shape appears when $g = \frac{\pi}{L}$. Combining this result with the auxiliary equation produces the expression for critical moment as shown in Eq. 33. With significant factoring and simplification Eq. 33 becomes Eq. 6, which presents Eq. 33 in terms of the critical moment.

$$\frac{\pi}{L} = \sqrt{-\frac{GJ}{2EC_w} + \sqrt{\left(\frac{GJ}{2EC_w}\right)^2 + \frac{m_x^2}{E^2 I_y C_w}}} \tag{33}$$

Moment Distribution Characterization

For circumstances where the applied moment m_x is not constant, as shown in Eq. 19, the moment function must be described continuously. In cases where the moment distribution is not continuous, it may be considered as piece wise continuous where a set of functions are used describe its effects. A simple moment distribution which corresponds to an applied end moment (m_0) is shown to see how Eq. 4 would be modified to accept a function for moment rather than a constant. The moment function for the end moment at the left end of a beam of length, *L* is shown in Eq. 34. Inserting

Eq. 34 into Eq. 4, results in the new governing differential stiffness equation as shown in Eq. 35.

$$m(z) = m_0\left(1-\frac{z}{L}\right) \tag{34}$$

$$EC_w\frac{d^4\phi}{dz^4} - GJ\frac{d^2\phi}{dz^2} - \frac{\left[m_0\left(1-\frac{z}{L}\right)\right]^2}{EI_y}\phi \tag{35}$$

Evidently the moment function may be inserted directly into the differential stiffness equation where the constant moment was previously present. Moment functions that are produced from an n^{th} degree spandrel distributed load type with possible end moments, as shown in Figures 8, 9, and 10, are described in Eq.'s 36, 37, and 38.

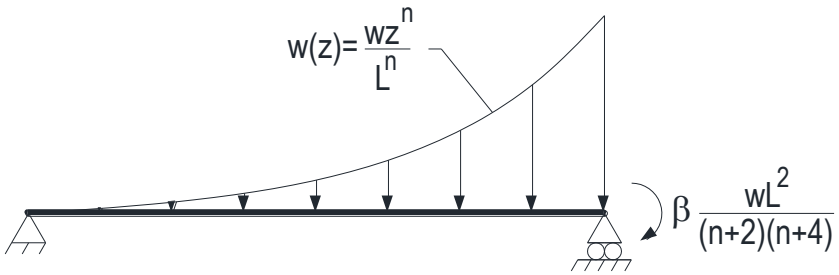

Figure 8: Spandrel load type with variable right end moment

$$m_x(z) = -\frac{wz^{n+2}}{(n+1)(n+2)L^n} + \left[\beta\frac{wL}{(n+2)(n+4)} + \frac{wL}{(n+1)(n+2)}\right]z \tag{36}$$

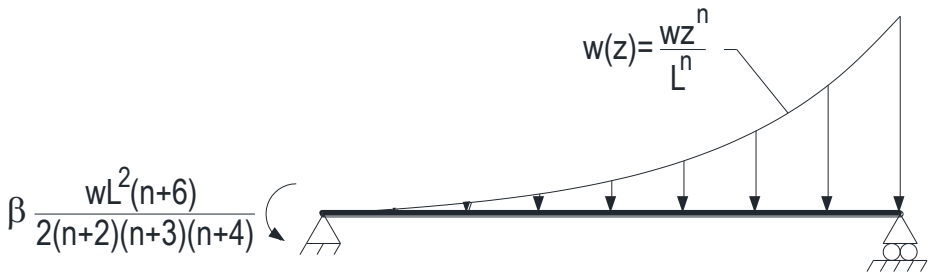

Figure 9: Spandrel load type with variable left end moment

$$m_x(z) = \frac{\beta wL(n+6)z}{2(n+2)(n+3)(n+4)} + \frac{wLz}{(n+1)(n+2)} - \frac{\beta wL^2(n+6)}{2(n+2)(n+3)(n+4)} - \frac{wz^{n+2}}{(n+1)(n+2)L^n} \quad (37)$$

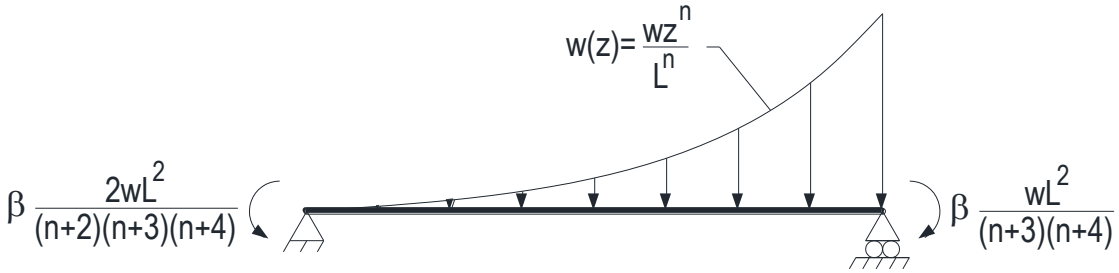

Figure 10: Spandrel load type with variable end moments

$$m_x(z) = -\frac{wz^{n+2}}{(n+1)(n+2)L^n} + \left[\beta\frac{2wL}{(n+2)(n+3)(n+4)} + \beta\frac{wL}{(n+3)(n+4)} + \frac{wL}{(n+1)(n+2)}\right]z \quad (38)$$

This spandrel type load distribution is selected, here, because by varying the linearity factor, *n*, other simpler load types can be recovered. These simpler distribution types that may be recovered correspond to a uniformly distributed load and a uniformly increasing load when n equals 0 and 1 respectively. The end moments applied are the same as the fixed end moment corresponding to each linearity factor, *n*. Additionally, the relative magnitude of this fixed end moment can be scaled according to the input

variable, β. The fixed end moments are calculated using the double integration method (Hibbeler 2009)

Effect of Load Height

In nearly all circumstances when flexural members are loaded, they are loaded at locations other than their shear center. This causes additional eccentricity when the cross section begins to undergo lateral torsional buckling, as illustrated in Figure 5. When the loading is not as shown in Figure 5 the expression is Eq. 14 changes. The additional twisting associated with this eccentricity for a more generalized load distribution is constructed based on the shear as the concurrent force as shown in Figure 11. Eq. 39 shows this additional twist with the variable $v_y(z)$ as the shear function.

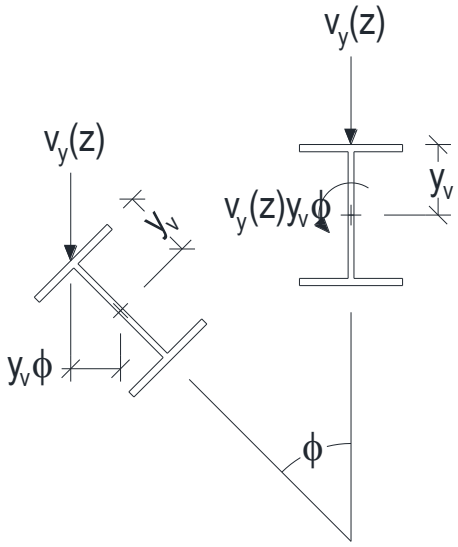

Figure 11: Eccentricity associated with shear loading above the shear center

$$m_{z'} = y_v v_y(z)\phi \tag{39}$$

Adding this component to the twisting causes Eq. 19 to change, reflecting the twist from load height, as shown in Eq. 40. Putting Eq. 40 in standard form allows stiffness properties for the weak axis of the beam to be used in the analysis. This may be seen in Eq. 41 as *E* (the modulus of elasticity) and I_y (the weak axis moment of inertia) enter in to the differential equation.

$$GJ\frac{d\phi}{dz} - EC_w\frac{d^3\phi}{dz^3} - y_v v_y(z)\phi = -\frac{dx}{dz}m_x \tag{40}$$

$$EC_w\frac{d^4\phi}{dz^4} - GJ\frac{d^2\phi}{dz^2} + y_v v_y(z)\frac{d\phi}{dz} - \frac{m_x^2(z)}{EI_y}\phi = 0 \tag{41}$$

The input functions of $v_y(z)$, for which there are many, in this study are based on the spandrel load type with end moments shown in Figures 8, 9, and 10 and corresponding to the moment functions in Eq.'s 36, 37, and 38. The shear functions corresponding to these moment functions in Eq.'s 36, 37, and 38 are shown in Eq.'s 42, 43, and 44 respectively. These shear functions must be used with the moment function that goes with it when inserted into Eq. 41. Furthermore, the shear functions cannot be for the reactive shear. They must be directionally correct in the analysis to be used as applied shear. A simple sign change from plus to minus is all that is needed to adjust for this effect. The change may be applied to the twisting component associated with the load height in the governing differential equation or in the shear functions themselves. The change was made in Eq. 41.

$$v_y(z) = -\frac{wz^{n+1}}{(n+1)L^n} + \beta\frac{wL}{(n+2)(n+4)} + \frac{wL}{(n+1)(n+2)} \tag{42}$$

$$v_y(z) = -\frac{wz^{n+1}}{(n+1)L^n} + \beta\frac{wL(n+6)}{2(n+2)(n+3)(n+4)} + \frac{wL}{(n+1)(n+2)} \tag{43}$$

$$v_y(z) = -\frac{wz^{n+1}}{(n+1)L^n} + \beta\frac{2wL}{(n+2)(n+3)(n+4)} + \beta\frac{wL}{(n+3)(n+4)} + \frac{wL}{(n+1)(n+2)} \tag{44}$$

CHAPTER 4 NUMERICAL METHOD

General

The elastic stiffness equation shown in Eq. 41 is difficult to solve analytically when the moment distribution is not constant and there is an applied shear load considered. To solve this differential equation a numerical method is used which considers the stiffness continuum as the summation of a series of finite difference elements. The numerical method used is a Taylor series polynomial expansion, with the expansion centered about each expansion point. Termed as a central difference approximation, the number of difference elements needed is determined by the convergence of the answer produced by the approximation.

Other methods are available to solve for the elastic lateral torsional buckling resistance of flexural members such as finite element modeling and energy methods, to name a couple. Using these methods are less desirable as they are not as versatile in adjusting for the various effects studied.

Central Difference Approximation

A Taylor series polynomial approximation is used to solve the differential equation shown in Eq. 41. The polynomial is expanded centrally about the point being characterized numerically to form a central difference approximation. The approximation (f_i), is dependent with respect to the approximate function $f(z_i)$ where the expansion point is characterized as $z_i = z^* + ch$ and $c = -\frac{N-1}{2},...,\frac{N-1}{2}$. This results in the

interpolation vector $\{(z_i, f_i)\}$ for which to solve the differential point by point. This can be seen illustratively in Figure 12.

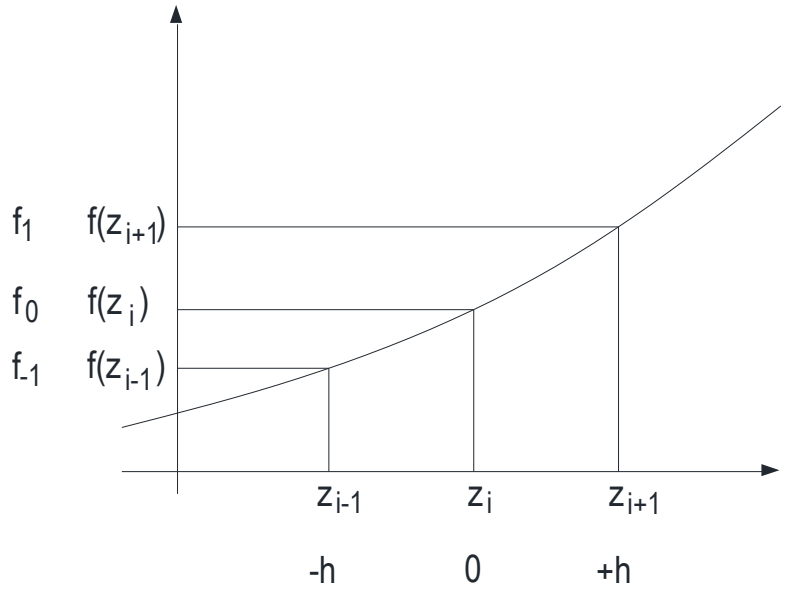

Figure 12: Central difference approximation for an arbitrary curve

To solve the 4th order differential equation in Eq. 41, an N-1 degree polynomial approximation requires that $N \geq 5$. The Taylor series takes the form as shown in Eq. 45 for each .expansion point (Nagle et al. 2004).

$$P_{N-1}(z) = \sum_{j=0}^{N-1} a_j z^j \tag{45}$$

To describe each differential operator in Eq. 41, Eq. 45 is differentiated so that instantaneously:

$$f^n(z^*) = P_{N-1}^n(z^*)$$

And,

$$P_{5-1}\left(z^{*}\right)=\sum_{j=0}^{5-1}a_{j}z^{j}=a_{0}+a_{1}z^{*}+a_{2}z^{*2}+a_{3}z^{*3}+a_{4}z^{*4}\Big|_{z^{*}=0}=a_{0} \tag{46}$$

$$P_{5-1}^{I}\left(z^{*}\right)=a_{1}+2a_{2}z^{*}+3a_{3}z^{*2}+4a_{4}z^{*3}\Big|_{z^{*}=0}=a_{1} \tag{47}$$

$$P_{5-1}^{II}\left(z^{*}\right)=2a_{2}+6a_{3}z^{*}+12a_{4}z^{*2}\Big|_{z^{*}=0}=2a_{2} \tag{48}$$

$$P_{5-1}^{III}\left(z^{*}\right)=6a_{3}+24a_{4}z^{*}\Big|_{z^{*}=0}=6a_{3} \tag{49}$$

$$P_{5-1}^{IV}\left(z^{*}\right)=24a_{4}\Big|_{z^{*}=0}=24a_{4} \tag{50}$$

Referring to Figure 12, the uniform distance (*h*) from the central expansion point is used to solve for the constants a_i*'s*. Because this distance h is constant, the constants may be solved for in relative proportion so that later in the numerical analysis, the distance h may be scaled to suit the number of expansion points used to describe the whole solution function. To solve for the first and second derivatives using the approximation, three terms are required. These terms correspond to *–h* from the expansion point located relatively at position 0, the position 0 itself, and a position *+h* from the expansion point located relatively at 0. This results in the system of equations to solve for a_i*'s* requiring only three terms, as follows:

$$P_{3-1}\left(-h\right)=f_{-1}=a_{0}-a_{1}h+a_{2}h^{2} \tag{51}$$

$$P_{3-1}\left(0\right)=f_{0}=a_{0} \tag{52}$$

$$P_{3-1}\left(h\right)=f_{1}=a_{0}+a_{1}h+a_{2}h^{2} \tag{53}$$

Solving for a_i's recovers expressions for a_0, a_1, and a_2.

$$a_0 = f_0 \tag{54}$$

$$a_1 = \frac{-f_{-1} + f_1}{2h} \tag{55}$$

$$a_2 = \frac{f_{-1} - 2f_0 + f_1}{2h^2} \tag{56}$$

To obtain the remaining constants within the context of the central difference approximation, five terms are required. The terms required correspond to *-2h*, *-h*, 0, *+h*, and *+2h*. The system of equations that results to solve for these remaining a_i*'s* are as follows:

$$P_{5-1}(-2h) = f_{-2} = a_0 - 2a_1h + 4a_2h^2 - 8a_3h^3 + 16a_4h^4 \tag{57}$$

$$P_{5-1}(-h) = f_{-1} = a_0 - a_1h + a_2h^2 - a_3h^3 + a_4h^4 \tag{58}$$

$$P_{5-1}(0) = f_0 = a_0 \tag{59}$$

$$P_{5-1}(h) = f_1 = a_0 + a_1h + a_2h^2 + a_3h^3 + a_4h^4 \tag{60}$$

$$P_{5-1}(2h) = f_2 = a_0 + 2a_1h + 4a_2h^2 + 8a_3h^3 + 16a_4h^4 \tag{61}$$

Solving for the remaining a_i*'s* (a_3 and a_4) yields the final expressions needed to describe Eq. 41 in numerical form.

$$a_3 = \frac{-f_{-2} + 2f_{-1} - 2f_1 + f_2}{12h^3} \tag{62}$$

$$a_4 = \frac{f_{-2} - 4f_{-1} + 6f_0 - 4f_1 + f_2}{h^4} \tag{63}$$

Using these constants, the differential operators in Eq. 41 may be described numerically as:

$$f\left(z^*\right) = a_0 = f_0 \tag{64}$$

$$f^{I}\left(z^*\right) = a_1 = \frac{-f_{-1} + f_1}{2h} \tag{65}$$

$$f^{II}\left(z^*\right) = 2a_2 = \frac{f_{-1} - 2f_0 + f_1}{h^2} \tag{66}$$

$$f^{III}\left(z^*\right) = 6a_3 = \frac{-f_{-2} + 2f_{-1} - 2f_1 + f_2}{2h^3} \tag{67}$$

$$f^{IV}\left(z^*\right) = 24a_4 = \frac{f_{-2} - 4f_{-1} + 6f_0 - 4f_1 + f_2}{h^4} \tag{68}$$

Using these operators to describe Eq. 41 produces the differential equation in numerical format, with $h = \frac{L}{m}$ where m is the number of segments used in the analysis.

$$\frac{EC_w}{h^4}\left(f_{-2} - 4f_{-1} + 6f_0 - 4f_1 + f_2\right) - \frac{GJ}{h^2}\left(f_{-1} - 2f_0 + f_1\right) + \frac{y_v v_y(i)}{2h}\left(-f_{-1} + f_1\right) - \frac{m_x^2(i)}{EI_y} f_0 = 0 \tag{69}$$

The boundary conditions shown in Eq.'s 26 and 27 in numeric form are as follows:

$$f_0 = 0, \quad \text{at} \quad i = \begin{Bmatrix} 0 \\ m \end{Bmatrix} \tag{70}$$

$$f_{-1} - 2f_0 + f_1 = 0, \quad \text{at} \quad i = \begin{Bmatrix} 0 \\ m \end{Bmatrix} \tag{71}$$

The numerical expression for the elastic stiffness shown in Eq. 69 can be arranged into a system of equations which are dependent on the number of expansion points. This system of equations takes the form $[c]\{f\} = 0$, where the value for the critical load is contained within the coefficient matrix $[c]$. Contained within this matrix are the numeric moment and shear functions. These functions are the same as those shown in Eq.'s 36, 37, and 38 for moment and Eq.'s 42, 43, and 44 for shear with the exception that they are transformed into numeric expressions discretized using the relation $z = \frac{iL}{m}$ for the independent variable *z* at each expansion point *i*. Here, *i* is the expansion point, *L* is the beam length and *m* is the number or segments used in the approximation. These moment and shear equations are shown in Eq.'s 72, 73, 74, 75, 76, and 77 respectively

$$m_x(i) = \frac{wL^2}{(n+1)(n+2)}\left[\frac{i\beta(n+1)}{m(n+4)} + \frac{i}{m} - \frac{i^{n+2}}{m^{n+2}}\right] \tag{72}$$

$$m_x(i) = \frac{wL^2}{(n+1)(n+2)}\left[\beta\frac{(n+1)(n+6)}{2(n+3)(n+4)}\left(\frac{i}{m} - 1\right) + \frac{i}{m} - \frac{i^{n+2}}{m^{n+2}}\right] \tag{73}$$

$$m_x(i) = \frac{wL^2}{(n+1)(n+2)}\left[\beta\frac{2(n+1)}{(n+3)(n+4)}\left(\frac{i}{m} - 1\right) + \beta\frac{(n+1)(n+2)i}{(n+3)(n+4)m} + \frac{i}{m} - \frac{i^{n+2}}{m^{n+2}}\right] \tag{74}$$

$$v_y(i) = \frac{wL}{(n+1)(n+2)}\left[1 + \beta\frac{(n+1)}{(n+4)} - \frac{i^{n+1}(n+2)}{m^{n+1}}\right] \tag{75}$$

$$v_y(i) = \frac{wL}{(n+1)(n+2)}\left[\beta\frac{(n+1)(n+6)}{2(n+3)(n+4)} + 1 - \frac{i^{n+1}(n+2)}{m^{n+1}}\right] \tag{76}$$

$$v_y(i) = \frac{wL}{(n+1)(n+2)}\left[1 + \beta\frac{2(n+1)}{(n+3)(n+4)} + \beta\frac{(n+1)(n+2)}{(n+3)(n+4)} - \frac{i^{n+1}(n+2)}{m^{n+1}}\right] \tag{77}$$

An example of how to generate this coefficient matrix $[c]$ is presented for a beam comprised of 2 finite difference elements. The coefficients in Eq. 69 are presented as constants to make the expression more compact. These constants are $a = \frac{EC_w}{h^4}$, $b = -\frac{GJ}{h^2}$, $c = \frac{y_v v_y(i)}{2h}$ and $d = -\frac{m_x^2(i)}{EI_y}$. The differential equation in numeric format at each expansion point *i* for 2 finite difference elements and boundary conditions is shown in the expression below.

$$\begin{aligned}
&i = 0 \rightarrow f_0 = 0\\
&i = 0 \rightarrow f_{-1} - 2f_0 + f_1 = 0\\
&i = 0 \rightarrow a(f_{-2} - 4f_{-1} + 6f_0 - 4f_1 + f_2) + b(f_{-1} - 2f_0 + f_1) + c(-f_{-1} + f_1) + df_0 = 0\\
&i = 1 \rightarrow a(f_{-1} - 4f_0 + 6f_1 - 4f_2 + f_3) + b(f_0 - 2f_1 + f_2) + c(-f_0 + f_2) + df_1 = 0\\
&i = 2 \rightarrow a(f_0 - 4f_1 + 6f_2 - 4f_3 + f_4) + b(f_1 - 2f_2 + f_3) + c(-f_1 + f_3) + df_2 = 0\\
&i = 2 \rightarrow f_2 = 0\\
&i = 2 \rightarrow f_{-1} - 2f_2 + f_3 = 0
\end{aligned} \tag{78}$$

The coefficient matrix $[c]$ that is produced from Eq. 78 is shown below.

$$[c]=\begin{bmatrix} 0 & 0 & 1 & 0 & 0 & 0 & 0 \\ 0 & 1 & -2 & 1 & 0 & 0 & 0 \\ a & (-4a+b-c) & (6a-2b+d) & (-4a+b+c) & a & 0 & 0 \\ 0 & a & (-4a+b-c) & (6a-2b+d) & (-4a+b+c) & a & 0 \\ 0 & 0 & a & (-4a+b-c) & (6a-2b+d) & (-4a+b+c) & a \\ 0 & 0 & 0 & 0 & 1 & 0 & 0 \\ 0 & 0 & 0 & 1 & -2 & 1 & 0 \end{bmatrix} \quad (79)$$

Setting the determinant of $[c]$ to zero allows the critical load w contained within the moment and shear functions in Eq.'s 72 through 77 to be solved as shown in Eq. 80.

$$\left|[c]\right| = 0 \quad (80)$$

CHAPTER 5 LOAD HEIGHT FACTORS FOR AISC STEEL BEAMS

Abstract

An analytical procedure is used to study the effects of moment distribution and load height on the elastic stability of AISC wide flange steel beams. Lateral torsional buckling is the limit state considered. Solutions are developed for a series of general moment distributions which are produced by continuous load types with possible end moments. For each load type, an equivalent uniform moment factor is developed. Additionally, a load height factor is developed to modify the equivalent uniform moment factor for these load types where loading is applied above the shear center. Solutions are processed numerically using a Taylor series polynomial approximation. Results are presented in terms of an equivalent uniform moment factor and a load height factor. Comparison with AISC code procedures for moment factor shows discrepancies that are conservative in some circumstances by approximately 51% and unconservative in others by approximately 8%. These differences appear to become amplified under the effect of reverse curvature bending and load position above the shear center. Results for load position show that members loaded above their shear center are more susceptible to lateral torsional buckling than those loaded at their shear center. Some design examples are presented using the load height factors developed.

Introduction

The existing analytical solutions describing lateral torsional stability provide coverage of a limited range of applicable design scenarios (Timoshenko and Gere 1961, Trahair 1998). Various additional studies have been performed to produce closed

form solutions based on analytical, numerical, and experimental data to estimate the lateral torsional buckling capacity of flexural members (Dumont 1937, Dumont and Hill 1940, Austin et al. 1955, Salvadori 1955, Clark and Jombock 1957, Nethercot and Trahair 1976, Kirby and Nethercot 1979, Suryoatmono and Ho 2002, Lopez et al. 2006, Serna et al. 2006, White and Kim 2008). These studies in general cover the distribution of moment between supports, load height with respect to the shear center, various levels of out of plane restraint at member ends, and buckling interaction (Wong and Driver 2010). To further study these effects, finite element, finite difference and other numerical methods have been employed. For example, finite element methods have been used by Serna et al. (2006) to study the effects of moment distribution between supports, while a finite difference approach was employed by Suryoatmono and Ho (2002) and Lopez et al. (2006) for the same purpose. Similarly, numerical methods have been used by Nethercot and Rockey (1972) to study the coupled effects of moment gradient and load height with respect to the shear center.

To account for the effect of moment distribution between supports, most approaches use an equivalent uniform moment factor to modify the capacity of flexural members loaded with nonuniform moment distributions. This factor is the ratio of the critical moment for a member with a particular moment distribution to the critical moment for the member with a uniform moment distribution (Wong and Driver 2010), where the critical moment refers to that which causes an instability failure. Two general approaches to develop closed form solutions for the equivalent uniform moment factor are presented in the literature. One is based on developing moment factors for specific load types (for example, a uniformly distributed load with variable end moments or a

concentrated load with variable end moments) (Austin 1961, Salvadori 1955, Clark and Hill 1960, Trahair 1998, Suryoatmono and Ho 2002), and the other for any arbitrary moment distribution (Kirby and Nethercot 1979, Serna et al. 2006). Typically, as might be expected, the moment factors developed for specific load types are more accurate than universal factors meant to describe a wider range of arbitrary moment distributions. Suryoatmono and Ho (2002) illustrate this variance in accuracy between the approaches for several closed form solutions of moment factor presented by various authors. Their results have generally shown that moment factor expressions based on arbitrary moment distributions produced generally conservative results, with some instances of unconservatism.

Another interest is the effect of load height with respect to shear center. Efforts that have considered this issue have coupled this effect with that of moment distribution between supports to produce one combined equivalent uniform moment factor (Nethercot and Rockey 1972). This results in expressions for moment factors at specific locations within the depth of the section which are typically provided at the shear center and the top and bottom flanges. Some design specifications simply neglect this effect entirely (AISC 360 2010, AASHTO 2012). For example, the prevailing US design specifications for steel structures and bridges, the American Institute of Steel Construction's Specification for Structural Steel Buildings, AISC 360 (AISC 2010) and the American Association of State Highway and Transportation Officials Load and Resistance Factor Design Bridge Design Specifications (AASHTO 2010), do not consider the effect of load height but provide a general expression for the effect of moment distribution between supports. The expression used in AISC 360 as well as

AASHTO is the same as that proposed by Kirby and Nethercot (1979) with slightly modified coefficients. Because the specifications for AISC and AASHTO are the same, reference to AISC will be used herein.

Despite the significant body of existing knowledge in this area, there are important details which have not been addressed. In particular, the precise account of the effects of a broad range of moment distributions as well as the effect of load height for these distributions. As noted above, although general solutions for arbitrary moment functions exist, the accuracy of this approach can be significantly improved, as will be shown below. To this end, the focus of this study is to accurately determine the effect on the lateral torsional stability of flexural members subjected to a set of moment functions for which precise solutions are currently unavailable. Additionally, a load position factor is developed to characterize the effect of load height on wide flange AISC steel sections. This load position factor is meant to modify the equivalent uniform moment factor for specific wide flange AISC sections. The moment functions considered are those produced by general, continuous type load distributions, as detailed below.

General Analytical Background

The governing differential equation representing the elastic stiffness of a flexural member under simple bending is produced by considering the rotational stiffness about each of the primary axes of the displaced (i.e. buckled) cross section (Timoshenko and Gere 1961, Trahair 1998). Combining expressions for Euler-Bernoulli bending about the *x* and *y* axes results in the well-known expression for lateral torsional buckling:

$$\frac{d^4\phi}{dz^4} - \frac{GJ}{EC_w}\frac{d^2\phi}{dz^2} - \frac{m_x^2}{E^2 I_y C_w}\phi = 0 \qquad (81)$$

Here, ϕ refers to rotation about the z-axis (i.e. twisting); E is Young's modulus; I_x and I_y are the strong and weak moments of inertia, respectively; G is shear modulus; J is the torsion constant; C_w is the warping constant; L is the length of the member; and m_x, m_y, and m_z represent the moments about the principle axes, such that $m_{x'} = m_x$, $m_{y'} = \phi m_x$, and $m_{z'} = -\frac{dx}{dz} m_x$.

The boundary conditions presented in this study are those associated with simple supports with twisting deformation fixed ($\phi = 0$) and warping free ($\frac{d^2\phi}{dz^2} = 0$) at the member ends.

For a particular member, the desired solution is generally the moment required to initiate lateral torsional buckling, or when the effective lateral and torsional stiffness of the system subtend to zero relative to the applied load. The solution for m_{0_cr}, the critical moment to cause lateral torsional buckling, can be determined for a simply supported member subjected to constant moment as (Timoshenko and Gere 1961, Trahair 1998):

$$m_{0\_cr} = \frac{\pi}{L}\sqrt{EI_y GJ\left(1 + \frac{EC_w}{GJ}\frac{\pi^2}{L^2}\right)} \qquad (82)$$

This critical moment applies for the case when a member is subjected to a constant moment function; for other moments, the result must be modified. The desire

here is to develop solutions for specific load types that have not yet been covered in literature sources to be used by typical design engineers.

The equivalent uniform moment factor (EUMF) for a particular load distribution is formulated by dividing the critical moment (m_{cr}) for that load type by the critical moment for a uniform moment distribution Eq. 83.

$$EUMF = \frac{m_{cr}}{m_{0\_cr}} \tag{83}$$

Considering moment equilibrium about the displaced cross section shows the effects of two different twisting effects. The twisting effect caused by the offset of the load height with respect to the shear center is denoted as $m_{z'v}$, while the twisting effect caused by an applied (non-uniform) moment distribution is denoted as $m_{z'b}$. The resistance of the member against these effects is denoted $m_{z'}$. Note a similar approach formulated for concentrated loads is presented by Trahair (1998). The resulting equilibrium equation is:

$$m_{z'v} + m_{z'b} - m_{z'} = 0 \tag{84}$$

where,

$$m_{z'v} = y_v v_y(z)\phi \tag{85}$$

$$m_{z'b} = -\frac{dx}{dz} m_x(z) \tag{86}$$

The variable y_v represents the distance from the load application point to the shear center of the member (upwards as positive), $v_y(z)$ is the shear force distribution

along the length of the member, and $m_x(z)$ is the moment distribution along the length of the member about the x-axis (strong axis).

Combining Eq.'s 84, 85, and 86 with the expression for Euler-Bernoulli bending (above) about the *y* axis forms the governing differential equation representing resistance to lateral torsional buckling considering the additional effects of non-uniform moment distribution and load height:

$$\frac{d^4\phi}{dz^4} - \frac{GJ}{EC_w}\frac{d^2\phi}{dz^2} + \frac{y_v v_y(z)}{EC_w}\frac{d\phi}{dz} - \frac{m_x^2(z)}{E^2 I_y C_w}\phi = 0 \qquad (87)$$

Note that in the third term, representing the twisting contribution from load height, the applied shear $v_y(z)$ is typically taken as a negative value to represent a force acting in the downward direction. The value of Eq. 87 is that it presents the applied shear as a continuous variable component. This allows for the substitution of general shear distributions into the expression. Moreover, it shows that the components for load height and moment distribution are independent, indicating that a separate factor for load height is obtainable that is not directly coupled to the component related to moment distribution. Thus, while the applied and reactive shear and moment distributions are of course directly related, the load height factor may be formulated with respect to either the shear or moment distribution. Inspection of Eq. 87 indicates that if $y_v>0$, the critical moment decreases as additional destabilizing twist is produced, whereas if $y_v<0$, the critical moment increases as the resulting twisting moment acts to resist the twist caused by the applied moment.

Because the load height and moment distribution components in Eq. 87 are independent, development of the load position factor is achieved by decoupling the effects of moment and load height. This is done by comparing the equivalent uniform moment factor for a beam loaded at its shear center to the same beam loaded at its top flange. The formulation for this load position factor, C_h is as follows:

$$C_h = 1 - \left(\frac{EUMF_0 - EUMF_f}{EUMF_0} \right) \tag{88}$$

The term $EUMF_0$ is the equivalent uniform moment factor for a member loaded at its shear center, for a specific load distribution. The term $EUMF_f$ is the equivalent uniform moment factor for the same member, but loaded at its top flange. Solution plots for C_h are shown below in the results section.

The load position factor, C_h is multiplied by the equivalent uniform moment factor for the load types studied in this paper to account for loading at the top flange (above the shear center). The nominal resistance for a member subject to elastic lateral torsional buckling loaded above its shear center is described in Eq. 89. The limit is set to $F_y S_x$ because the analysis is for elastic behavior only.

$$R_n = C_h M_{0\_cr} (EUMF_0) \leq F_y S_x \tag{89}$$

Solution Procedures

Solving the differential equations representing lateral torsional stiffness analytically is difficult and in some cases may be impossible. Therefore, alternative numerical methods have been used to produce approximate solutions. For example, a

finite difference approach was used by Suryoatmono and Ho (2002), while finite element methods have also been considered (Wang et al. 2012).

In this study, a finite difference approach is used to solve Eq. 87. The approach uses a central difference approximation considering the first non-zero terms of a Taylor series polynomial expansion to describe the differential operators. The twisting deformation (ϕ) is approximated by the quadratic polynomial *f(z)*. The *N*-1 degree polynomial approximation has the form $P_{N-1}(z)=\sum_{j=0}^{N-1}a_j z^j$, where the differential operators $\frac{d^n\phi}{dz^n}$ may then be expressed in terms of the polynomial approximation (Nagle et al. 2004). For example, the first term becomes

$P_{5-1}(z)=\sum_{j=0}^{5-1}a_j z^j=\left(a_0+a_1 z+a_2 z^2+a_3 z^3+a_4 z^4\right)\Big|_{z=0}=a_0$, while the last term is: $P_{5-1}^{IV}(z)=\left(24a_4\right)\Big|_{z=0}=24a_4$ (intermediate terms not shown for brevity).

Constants a_i's may then be solved for in order to write the differential operators in numerical form $f_i=f(z_i)$. For example, the first term becomes $f(z)=a_0=f_0$, while the last term is $f^{IV}(z)=24a_4=\frac{f_{-2}-4f_{-1}+6f_0-4f_1+f_2}{h^4}$.

Applying the numerical operators to Eq. 87 produces the governing differential equation for lateral torsional stiffness including non-uniform moment and load height effects in numerical format (Eq. 90):

$$EC_w\left(\frac{f_{-2}-4f_{-1}+6f_0-4f_1+f_2}{h^4}\right)-GJ\left(\frac{f_{-1}-2f_0+f_1}{h^2}\right)+y_v v_y(z)\left(\frac{-f_{-1}+f_1}{2h}\right)-\frac{m_x^2(z)}{EI_y}(f_0)=0 \qquad (90)$$

To transform the moment ($m_x^2(z)$) and shear ($v_y(z)$) functions into numerical form, the variable z is discretized at each expansion point (not including expansion points at boundary conditions) as: $z = i\Delta z = \frac{iL}{m}$, where m is the number of discretized segments for the beam length considered.

Once discretized, Eq. 90 can be expressed as a series of algebraic equations $[c]\{f\}=0$, where the critical load of interest is contained within the coefficient matrix $[c]$. In this case, the smallest load that allows the determinant of $[c]$ to equal zero indicates the critical load for the system. The value solved for is the independent variable component to the moment and shear functions, represented as w. Examples of this for both moment and shear a provided below in Eq.'s 92 and 93.

Convergence of the solutions is achieved by increasing the number of segments m used in the analysis and comparing the critical moment to subsequent results. When the difference in results becomes sufficiently small (taken as less than 0.5%) the solution has converged. In general, this required 40 segments. To verify the validity of the approach, some cases with known solutions (for example, a simply supported member with a uniformly distributed load, as well as that with equal and unequal end moments applied) were considered and compared to the analytical solutions. All test cases considered produced matching results to the known solutions (Timoshenko and Gere 1961, Trahair 1998).

Load Distributions Considered

Previous studies provide a range of different moment distributions and their effects on lateral torsional buckling. There are a total of 12 such distributions previously studied, and are summarized by Wong and Driver (2010). In general, these cases include combinations of uniform loads, concentrated loads and end moments, with simple support conditions and loading at the shear center.

In this study, a more generalized moment distribution is considered, which can model a wider variety of load possibilities; in particular, an n^{th}-degree spandrel distributed load with possible end moments, as shown in Figure 1. For this load distribution type, fixed end moments are considered at both ends and each end individually to produce a comprehensive range of results. The spandrel load itself is described as:

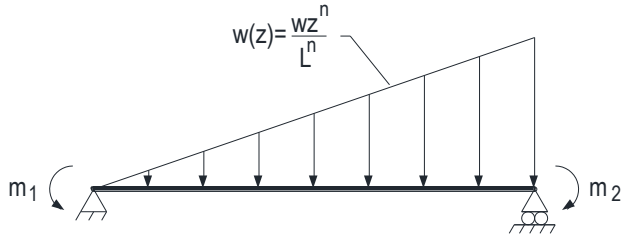

$$\text{Type 1: } m_1 = 0,\ m_2 = \beta \frac{wL^2}{(n+2)(n+4)}$$

$$\text{Type 2: } m_1 = \beta \frac{wL^2(n+6)}{2(n+2)(n+3)(n+4)},\ m_2 = 0$$

$$\text{Type 3: } m_1 = \beta \frac{2wL^2}{(n+2)(n+3)(n+4)},\ m_2 = \beta \frac{wL^2}{(n+3)(n+4)}$$

Figure 13: Load types studied

$$w(z) = \frac{wz^n}{L^n} \tag{91}$$

Note that when *n=0*, a simple beam with uniform load (and possible end moments) is recovered, and when *n=1*, a linearly increasing (triangular) distributed load is obtained. For cases where *n>1*, the load distribution becomes increasingly nonlinear as *n* increases. To solve Eq. 88 with the loads shown in Figure 13, the corresponding moment and shear equations are transformed into numerical form, as previously described. For example, the resulting shear and moment equations for Type 1 in Figure 13 are:

$$v_y(z) = -\frac{wz^{n+1}}{(n+1)L^n} + \beta\frac{wL}{(n+2)(n+4)} + \frac{wL}{(n+1)(n+2)} \tag{92}$$

$$m_x(z) = -\frac{wz^{n+2}}{(n+1)(n+2)L^n} + \left[\beta\frac{wL}{(n+2)(n+4)} + \frac{wL}{(n+1)(n+2)}\right]z \tag{93}$$

Numerically, where $z = \frac{iL}{m}$:

$$v_{y,i} = \frac{wL}{(n+1)(n+2)}\left[1 + \beta\frac{n+1}{n+4} - \frac{i^{n+1}(n+2)}{m^{n+1}}\right] \tag{94}$$

$$m_{x,i} = \frac{wL^2}{(n+1)(n+2)}\left[\frac{i\beta(n+1)}{m(n+4)} + \frac{i}{m} - \frac{i^{n+2}}{m^{n+2}}\right] \tag{95}$$

In these expressions, β is an indexing factor that allows the fixed end moments to be arbitrarily increased or decreased.

Current Code Procedures

To understand the current practice used to determine the elastic stability of flexural members as loaded in Figure 13; specifications from the AISC 360 are compared with numerical results. Numerical results for different load height are not directly compared to AISC because they do not have provisions covering this effect. The code comparison effort is to show deviation from the moment factor for the load types described in this paper.

An equivalent uniform moment factor is used. AISC 360 only considers the distribution of moment between supports, whereas provisions for other effects are not specifically addressed. In AISC 360, an equivalent (in terms of critical moment) uniform moment factor is developed by considering the absolute values of the maximum moment M_{max}, and the quarter points moments M_a, M_b, and M_c, within the span, where the moment factor is expressed as:

$$C_b = \frac{12.5M_{max}}{2.5M_{max} + 3M_a + 4M_b + 3M_c} \tag{96}$$

Eq. 96 is similar to that proposed by Kirby and Nethercot (1979) with the coefficients slightly adjusted to more accurately describe the effects for a beam with fixed ends. Eq. 96 is applicable to general moment distributions with the exception of cantilever members where the free end is unbraced. In this case, the moment factor $C_b = 1.0$.

Results and Code Comparison

The three load distributions shown in Figure 13 are applied to an example beam (W14x132) spanning 30 feet. Because the results are normalized by using the equivalent uniform moment factor approach, these plots will remain approximately the same for reasonable input values of *E, I, G, and J* (i.e. any reasonable beam size). This is recognized in design specifications as the same process is used for equivalent uniform moment factor regardless of beam size. Note that this assumes that the input parameters will allow the beam to buckle elastically. In this study, the fixed end moment index, β, is varied from -2 to 2 to represent cases for applied end moments found with simply supported ends. The linearity factor, n, is varied discretely from 0 to 2 to present a range of solutions for the load and end moment configuration considered. The results are found by first determining the critical load intensity, w, which causes instability for the case considered (see Eq's. 94 and 95). This critical load (w_{cr}) is then transformed into a moment (m_{cr}), and then divided by the critical moment obtained from Eq. 82 (m_{0_cr}). This ratio (m_{cr}/m_{0_cr}) is the equivalent uniform moment factor.

Figures 14 presents the equivalent uniform moment factor for distribution Types 1-3 with *n=0,1* and *2* for members loaded at their shear centers. Figures 15-23 present load height factor results for load Types 1-3 and variable load heights. The equivalent uniform moment factor and load height factor are plotted against the end moment factor, β. In these plots, the load height factor is plotted against the end moment factor for load heights at 6, 9, 12, 15, 18, and 22in above the shear center. These load heights correspond to AISC beams by section depth W12, W18, W24, W30, W36, and W44 respectively considering the member loaded at its top flange. These results for load

height factors also apply for members with loading is above the top flange but only up to 22in above the shear center.

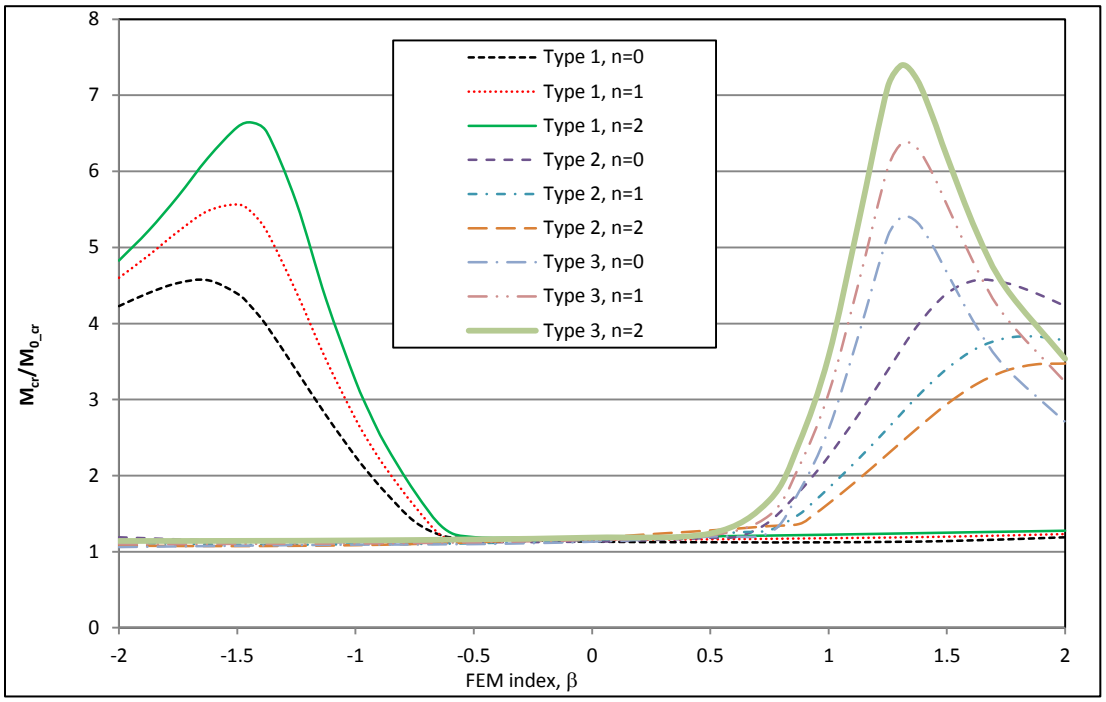

Figure 14: Load Types 1-3 solution plot, Yv=0

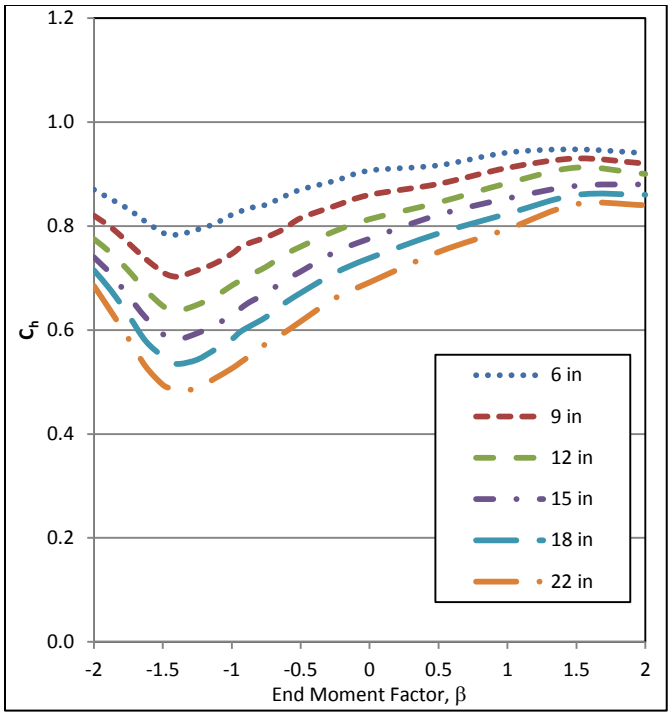

Figure 15: Load Type 1 load height factors, n=0

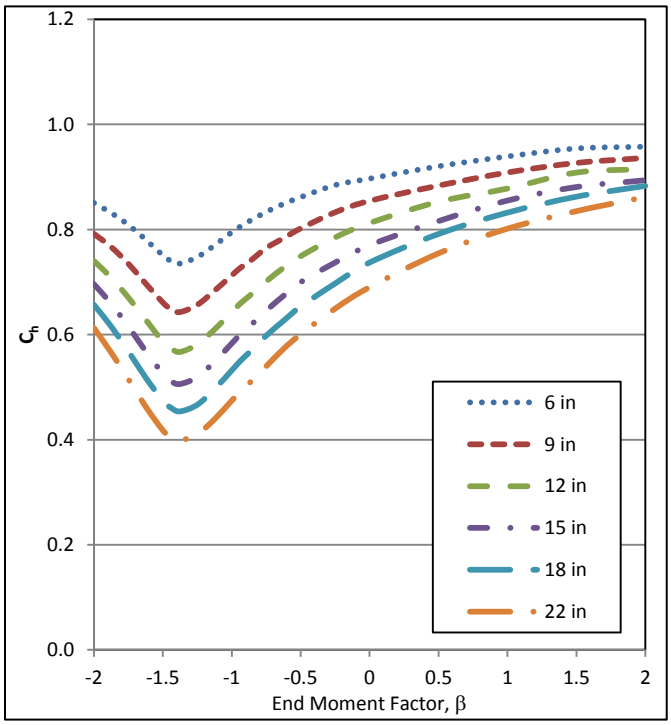

Figure 16: Load Type 1 load height factors, n=1

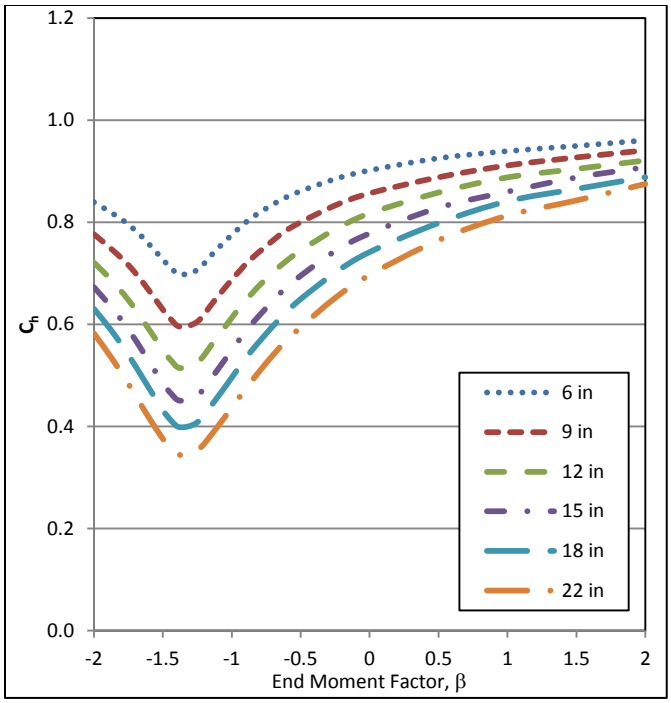

Figure 17: Load Type 1 load height factors, n=2

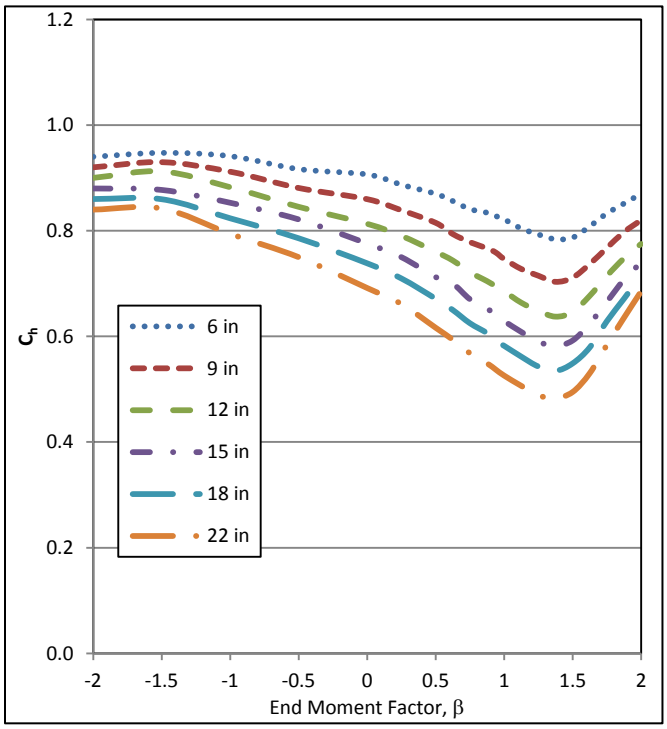

Figure 18: Load Type 2 load height factors, n=0

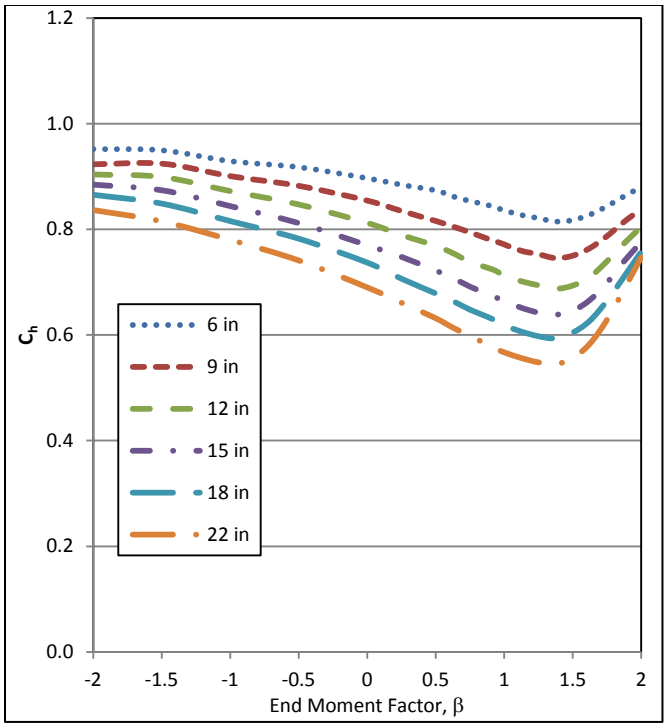

Figure 19: Load Type 2 load height factors, n=1

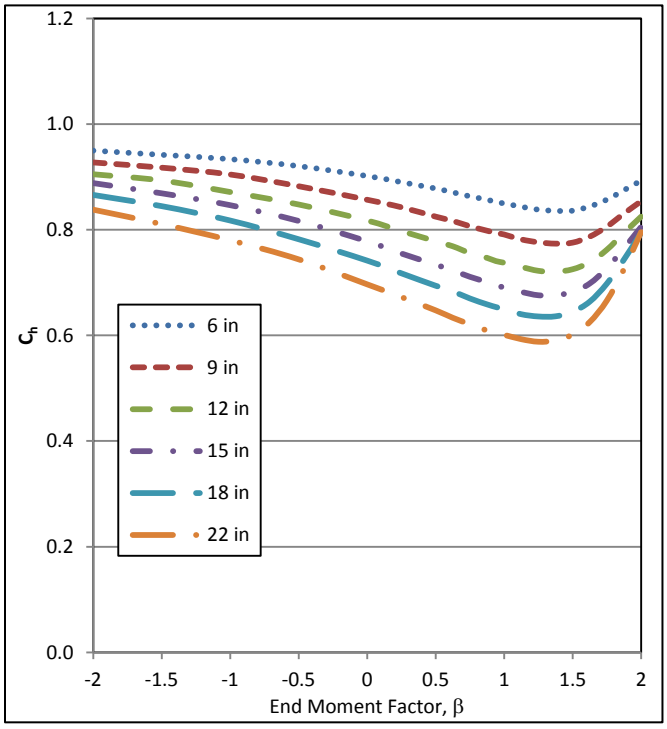

Figure 20: Load Type 2 load height factors, n=2

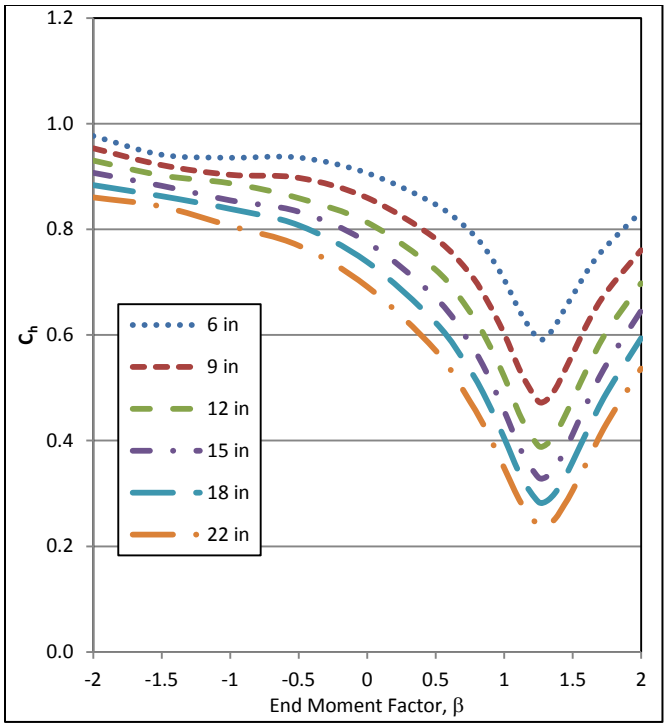

Figure 21: Load Type 3 load height factors, n=0

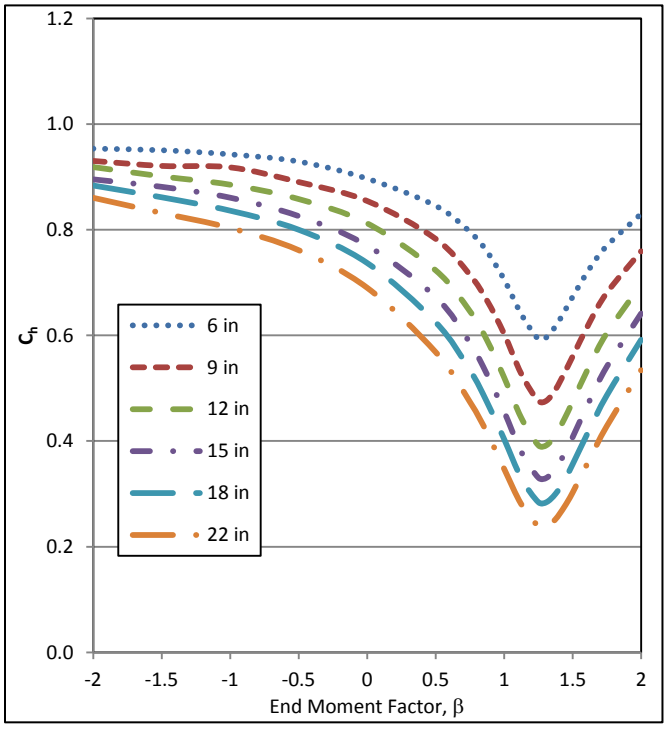

Figure 22: Load Type 3 load height factors, n=1

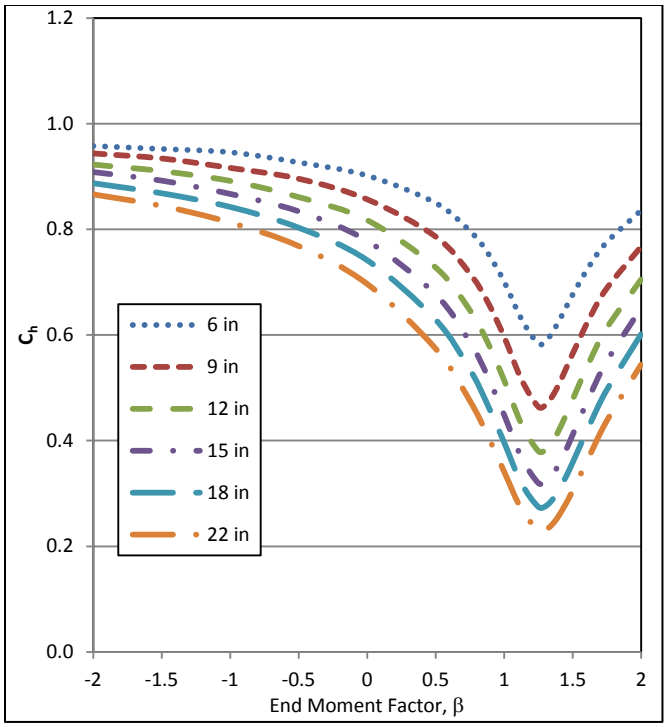

Figure 23: Load Type 3 load height factors, n=2

It can be observed in that when *n=0* and y_v*=0*, a uniformly distributed load is recovered with variable end moments. This distribution type has been studied in depth by others, and the results obtained for these curves match those found elsewhere (Suryoatmono and Ho 2002, Lopez et al. 2006, Serna et al. 2006).

The other results presented are for a uniformly increasing load with end moments *(n=1)* and for a parabolic load (*n=2)*. Inspection of Figure 14 shows that when the end moment factor approaches values that cause reverse curvature bending (i.e. when $\beta \leq 0$ for distribution Type 1 and when $\beta \geq 0$ for distribution Types 2 and 3), the equivalent uniform moment factor increases. Otherwise, the effect of the fixed end moments is negligible. The effect of load height shown in Figures 15-23 is as expected; when the member is loaded above the shear center, the capacity of the member to resist lateral

torsional buckling decreases. For end moment factors $\beta < 0$ for Type 1 loading and $\beta > 0$ for Types 2 and 3 loadings, the change in capacity due to the vertical position of the load can become large, showing particularly high reductions in lateral torsional buckling capacity when the load is placed above the shear center.

For comparison, solutions provided by AISC 360 are presented in Figures 24, 25 and 26 along with the numerical solutions found in this study for a member loaded at the shear center. It was found that in general, for end moment factors greater than -0.5 for Type 1 loading and for factors less than 0.5 for loading Types 2 and 3, the code expressions well match the theoretical solutions. However, outside of these ranges, large differences may result, where code predictions may be very conservative, and in some cases, overestimate capacity. In particular, the code specifications begin to display significant discrepancies from the true solution in some regions of reverse curvature bending (i.e. when both positive and negative moments appear on the span). For distribution Type 1, meaningful discrepancies begin to occur where $\beta < -0.5$ (Figure 24), while for distribution Types 2 and 3, code results diverge significantly from the true solution when $\beta > 0.5$ (Figures 25 and 26).

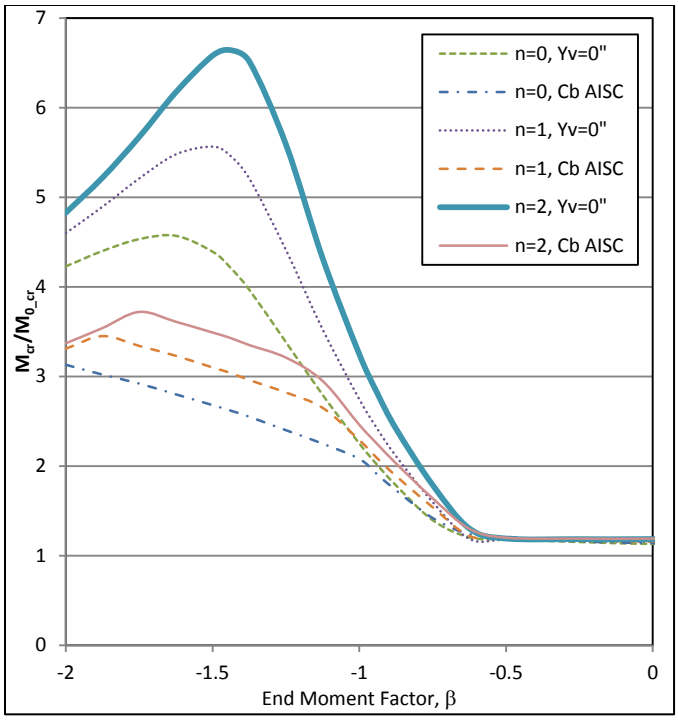

Figure 24: Load Type 1 code procedure comparison, n=0, 1 and 2

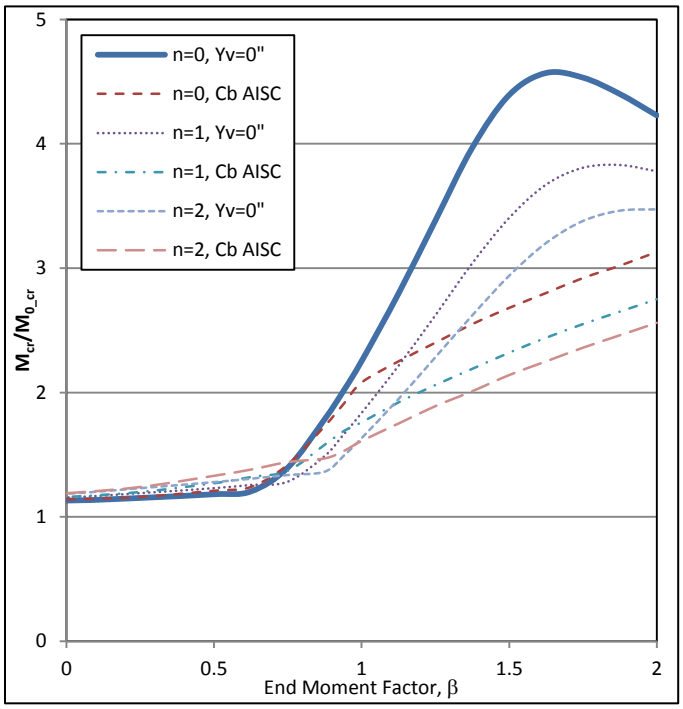

Figure 25: Load Type 2 code procedure comparison, n=0, 1 and 2

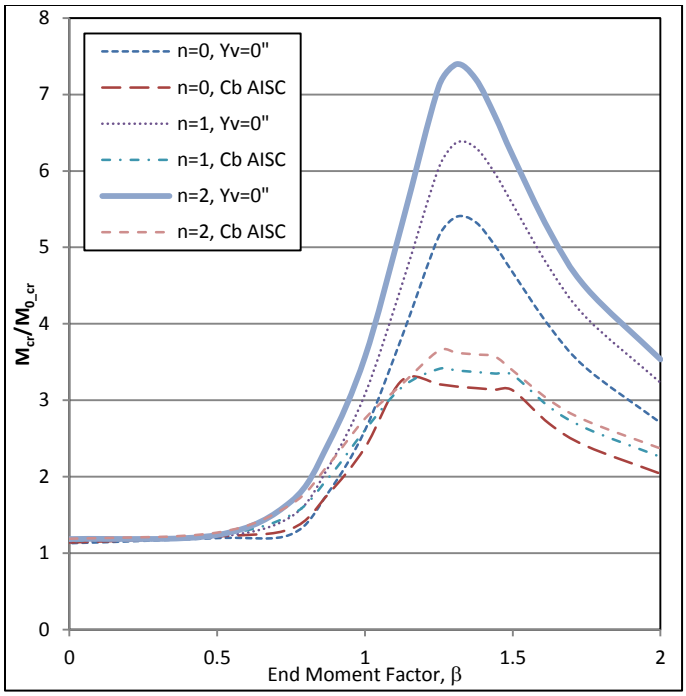

Figure 26: Load Type 3 code procedure comparison, n=0, 1 and 2

The conclusion from this data is that the closed form solution for moment factor used by AISC is inadequate for some load types and should be replaced by moment factors that are tailored to these specific load types. Additionally, because AISC does not address load height factors, the codified results obtained for the lateral torsional buckling limit state are very unconservative in circumstances where members are loaded above their shear center.

Practical Design Example

To utilize this work for design purposes an example is shown considering a W18x106 simply supported, spanning 30 feet, subject to Type 3 loading with *n=0*, and an end moment factor of 0.875. A992 steel is considered. The limit state is elastic lateral torsional buckling with the effects of load height and moment distribution between

supports considered. First the basic strength of the W18x106 is determined by using Eq. 82. This basic strength is then modified by the equivalent uniform moment factor and the load height factor. These factors are read directly from Figure 14 and Figure 21 respectively. Once each of these values is obtained, Eq. 89 is used to determine the nominal moment capacity of the beam, limited to the elastic moment. The results for each step are presented in Table 3. It should be noted that for a particular member, half the beam depth is appropriate for the load height above the shear center. For this case, the member is a W18 which has a shear center located 9in below the top flange; therefor the 9in curve is used. For beam depths that fall between those that are listed, linear interpolation may be used to approximate the equivalent uniform moment factor and the load height factor. Furthermore, this same method may be used for load situations where loading is above the top flange of the beam, but within 22in of the shear center.

m_{0_cr} (in-k)	EUMF	C_h	F_yS_x	R_n (in-k)
7705	1.79	0.67	10200	9241

Table 3: Design example results

Need for Further Work

To the extent of load height factors, more work is needed. The load distributions studied in this paper only cover a small range of those scenarios seen in typical design. The load types summarized by Wong and Driver (2010) provide an example of

additional distributions to be characterized, among other more exotic types such as those produced by design trucks on bridges and nonlinear aerodynamic loads on building components and cladding. Other work is needed to characterize these load height factors for members under alternative restraint conditions including end supports and continuous and discrete bracing. Exotic beam types also need characterized such as those with copes and other unstiffened elements.

Conclusion

An analytical procedure is formulated to describe the effects of moment distribution and load height on the elastic stability of flexural members. Lateral torsional buckling is the limit state considered. Solutions for a series of general moment distributions are developed for n^{th} degree spandrel type distributed loads with fixed end moments. The height of the load with respect to the shear center is varied to correspond to a range of AISC wide flange steel beams. Solutions are processed numerically using a Taylor series polynomial expansion. Results are presented in terms of an equivalent uniform moment factor, and a load height factor.

The load types studied are intended to add to the database of established results. The flexibility of the spandrel-type solutions allows consideration of a wide range of continuous loads, including uniformly distributed and increasing load distribution types with variable fix end moments. Based on the data presented in this paper up to $n=2$, the equivalent uniform moment factor and shear factor can be read from the figures for specific values of n, y_v and β .Solutions show that current code procedures have significant discrepancies in capacity prediction for the ranges of fixed

end moment discussed above. For loading at the shear center, comparison against code procedures reveals discrepancies that are conservative in some circumstances by approximately 51% and unconservative by approximately 8%. These differences appear to become amplified as reverse curvature bending becomes more pronounced. In general, for distribution Type 1, significant differences from code procedures appear when $\beta < -0.5$, while for distribution Types 2 and 3, differences become significant when $\beta > 0.5$.

The results also show that the effect of load height causes large changes in capacity for AISC steel beams. As expected, loading above the shear center causes a reduction in capacity. Load height factors are provided for AISC wide flange beams W12 through W44. These factors are a numerical approximation of the exact solution for an elastically buckling beam.

CHAPTER 6 ADDITIONAL ELASTIC STABILITY DEVELOPMENTS

Introduction

Other developments in the elastic stability of flexural members are important to note, particularly those that relate to the level and type of restraint provided by both continuous and discrete bracing mechanisms. These bracing mechanisms are those associated with flooring systems, the way in which the load is applied, and point braces applied at specific locations along the length of the beam.

Restraint from Applied Loads

When loads are applied to flexural members there may be a tendency for these loads to restrain the cross section from displacing laterally and torsionally by the way the load connects to the member it is loading. This effect is mainly prevalent when members are not designed as part of a system connected by a diaphragm type structure to distribute the load and when members are in the construction phase where they often are loaded individually by workers, equipment and construction materials. Additionally when joists are framed into a collector girder the joists that are applying the load to the collector girder act to restrain the collector girder by their level of connectivity.

To understand the effect of restraint from applied loads, a free body diagram is developed to illustrate how the load acts on the cross section as shown in Figure 27.

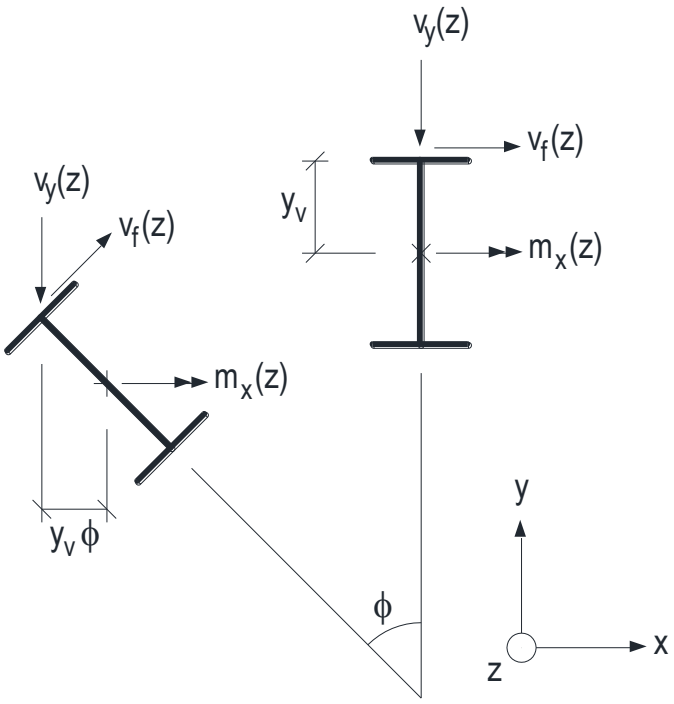

Figure 27: Restraining force from applied load

As shown in Figure 27, the restraining force is provided by the imposing shear load to the beam, normal to the direction in which it is applied. This indicates that the level of connectivity between the load and the member directly influences the restraint effect. For circumstances where the load is connected using standard structural connection methods (bolting and welding) the level of connectivity is the maximum available which is related to the size of the load and the stiffness of the connecting member which is applying the load. For circumstances where the load is not applied by structural connectivity methods, a friction factor is considered. This is appropriate because there may not be a member applying the load and if there is, a resting friction connection is not suitable to resist lateral or torsional movement by any means (stiffness) other than the friction that exists between the surfaces.

To describe this effect equilibrium equations are composed with the lateral friction force opposing the twisting stiffness $m_{z'}$, as shown below.

$$m_{z'} = m_{z'v} - m_{z'f} + m_{z'b} \tag{97}$$

$$m_{z'f} = y_v \mu_L \phi v_y(z) \tag{98}$$

$$GJ\frac{d\phi}{dz} - EC_w\frac{d^3\phi}{dz^3} = m_{z'b} + m_{z'v} + m_{z'f} \tag{99}$$

The term $m_{z'f}$ refers to the rotational component caused by the friction force. As shown in Eq. 98 this imposed force is related to the friction coefficient between the load and the member μ_L. Otherwise, this term is the same as the rotational force produced by the load height as described by $m_{z'v}$ however acting in the opposite direction. Because this interdependence between the shear force causing load height twisting and the shear force imposed friction force causing twisting, the term $\mu_L - 1$ appears in the governing differential equation, shown in Eq. 100.

$$\frac{d^4\phi}{dz^4} - \frac{GJ}{EC_w}\frac{d^2\phi}{dz^2} - \frac{(\mu_L - 1)y_v v_y(z)}{EC_w}\frac{d\phi}{dz} - \frac{m_x^2(z)}{E^2 I_y C_w}\phi = 0 \tag{100}$$

Numerical methods are the best option to solve Eq. 100. The same method that is proposed in Chapter 4 is suitable and the numeric version is shown in Eq. 101.

$$EC_w\left(\frac{f_{-2} - 4f_{-1} + 6f_0 - 4f_1 + f_2}{h^4}\right) - GJ\left(\frac{f_{-1} - 2f_0 + f_1}{h^2}\right) - (\mu_L - 1)y_v v_y(z)\left(\frac{-f_{-1} + f_1}{2h}\right) - \frac{m_x^2(z)}{EI_y}(f_0) = 0 \tag{101}$$

This numeric expression can be arranged into a system of equations dependent on the number of expansion points as described by Eq. 78.

Restraint Provided by Continuous Sources

In much the same way, Eq. 100 may be altered for continuous restraint situations where the restraint applied is insufficient to restrain buckling. Such situations can arise from thin membranes attached to systems of members such as fabrics intended to block wind loading. These membranes are in some situations insufficient to provide restraint to prevent the members attached to it from buckling. Eq. 100 may be altered so that instead of a friction force imposed by the applied shear load, as shown in Figure 27, a stiffness function for the membrane may be substituted. The stiffness function would need to have components representing the rotational stiffness of the membrane and the lateral stiffness. Figure 28 illustrates how the continuous restraint would be applied, shown as the function $r_x(z)$.

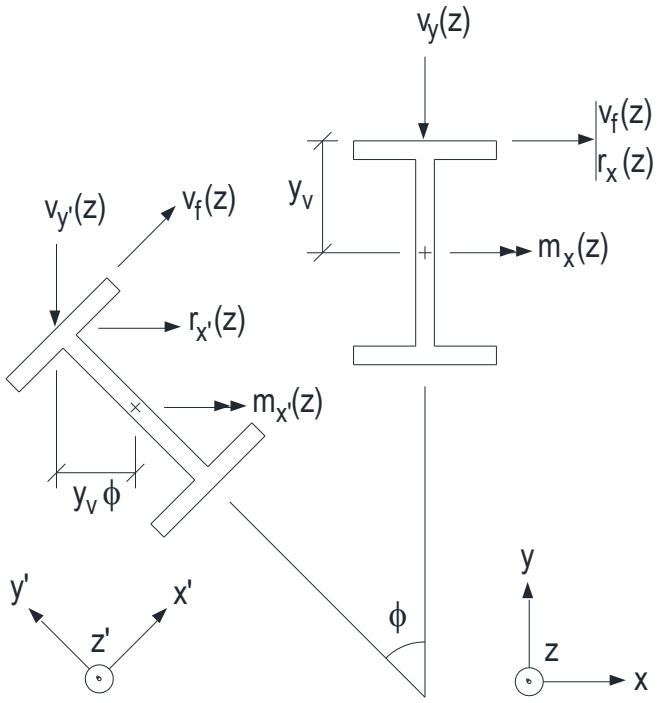

Figure 28: Restraint provided by continuous sources

Restraint Provided by Discrete Torsional Braces

Discrete torsional braces may be applied at any location along the length of the member under consideration to improve its capacity. Torsional braces do not act to restrain the lateral displacement of the cross section but instead constrain rotation at the location of the brace. A situation where a brace is likely to act as a torsional brace as opposed to a lateral-torsional brace is when a system of discretely braced members all buckle in the same direction at the same time i.e. roof trusses failing due to wind loading. The braces in these circumstances are most certainly lateral-torsional braces, but due to the way the structure fails, they are only able to resist torsional forces, Figure 29 illustrates a discrete brace at some location ψ along the length of a member.

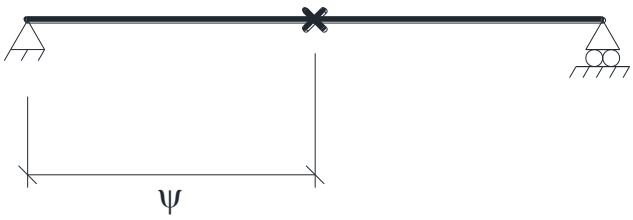

Figure 29: Discrete torsional brace

To include this torsional brace in the analysis it is handled in much the same way as the boundary conditions shown in Eq.'s 26 and 27. The condition imposed at the brace location ψ, is for torsion fixed and warping free. The constraints are written as follows:

$$\phi = 0, \quad \text{at} \quad z = \psi \tag{102}$$

$$\frac{d^2\phi}{dz^2} = 0, \quad \text{at} \quad z = \psi \tag{103}$$

These may be transformed into numerical expression and input into the coefficient matrix $[c]$ (shown in Eq. 79) to solve for the critical load. It should be noted that if this numerical method proposed above is used, the brace must coincide with the location of an expansion point otherwise there is no accurate place for it in the coefficient matrix $[c]$.

CHAPTER 7 RELIABILITY OF BEAMS SUBJECT TO ELASTIC LTB

Abstract

A reliability analysis of steel beams subjected to lateral torsional buckling is presented. This involves setting up a load model and establishing a resistance model considering lateral torsional buckling as the limit state. Resistance is modeled using an analytical approach to calculate equivalent uniform moment factors for different load distributions. The equivalent moment factors are calculated considering the effects of load height. The reliability analysis is conducted using a Monte Carlo Simulation and results are reported in terms of reliability index β. The results indicate that for most cases, reasonably uniform levels of reliability with regard to lateral torsional buckling are obtained with beams designed using AISC 360 specifications. However, in cases of reverse curvature bending, the AISC 360 specifications tend to underestimate actual safety level, in some cases significantly. It was also observed that for positive load heights, the AISC 360 specifications overestimate safety level, whereas for negative load heights, safety is underestimated.

Introduction

A wide range of literature describing the lateral torsional buckling (LTB) behavior of structural steel beams based on analytical, numerical and experimental data is currently available (Dumont 1937, Dumont and Hill 1940, Hill 1954, Austin et al. 1955, Salvadori 1955, Clark and Jombock 1957, Nethercot and Trahair 1976, Kirby and Nethercot 1979, Suryoatmono and Ho 2002, Lopez et al. 2006, Serna et al. 2006, White and Kim 2008). Moment distribution between the supports, effect of load height with

respect to shear center, buckling interaction, and out-of-plane restraints at member ends are some of the common issues considered while studying the lateral torsional stability of beams. Two of the primary considerations, moment distribution between supports and placement of load height with respect to shear center, are further discussed below.

For flexural members loaded with non-uniform moment distributions, an equivalent uniform moment factor approach is often considered. This factor is the ratio of the critical moment for a member with a particular moment distribution to the critical moment for the member with a uniform moment distribution (Wong and Driver 2010), where the critical moment refers to that which causes an instability failure. The work of various researchers has developed this concept. For example, Nethercot and Rockey (1972) used numerical data in an effort to describe a general procedure to determine the elastic critical moment of beams. Much more recently, Suryoatmono and Ho (2002) used a finite difference technique to solve the governing differential equation for elastic stiffness, and have shown that the results produced by the AISC equivalent uniform moment factor are unconservative in some circumstances.

To consider the effect of load height with respect to shear center, past research has coupled this effect with that of moment distribution between supports to produce a combined equivalent uniform moment factor (Nethercot and Rockey 1972). This resulted in moment factor expressions for different load placement depths (in the vertical direction) on the beam cross-section, where results are usually presented for loads placed the shear center and at the top and bottom flanges. The difference in moment factor values due to the load height effect, in practice, become amplified as the

members depth deviates from the depth of the members used in the study. This essentially means that because the load height effect was not considered, the numerical curve fitting that was used to create the moment factors is skewed based on the actual members depth compared to that depth of the member used to produce the numeric data. Coupling load height and moment distribution effects into one normalized factor, the equivalent uniform moment factor, causes this issue to become prevalent in state of the practice design culture as load heights are not specifically addressed. Coupling these effects from numeric data can also be dangerous especially during erection when members may be temporarily braced and often see near maximum loads from construction equipment and materials.

Despite the research conducted on this issue, it can be observed that some design specifications such as American Institute of Steel Construction 360 (AISC 2010) and the AASHTO LRFD Bridge Design Specifications (AASHTO 2012) have neglected the effect of load height while estimating the equivalent moment factor. The expressions provided for the equivalent moment factor in these design specifications implicitly consider loads to be acting at the shear center, neglecting the effect of load height throughout the depth of the cross-section. Moreover, the equivalent moment factor expressions used in these design specifications use a general closed form expression which, for some load scenarios, produces significantly unconservative results. A potential solution to this issue is to produce moment factor values for specific moment distributions and load heights. This approach is further described in the 'Resistance Model' section, below. As noted above, a significant body of literature is available that addresses LTB. However, few studies have investigated the failure probability of

structural steel members with regard to LTB. Ellingwood et al. (1980) and Galambos (REF) developed initial resistance statistics for LTB, while more recently, a statistical evaluation of LTB resistance of steel I-beams for Eurocode is presented by Robelo et al (2008), wherein a new partial safety factor was proposed. Szalai and Papp (2008) presented a new probabilistic evaluation of standard resistance models for the stability of columns and beams, while Badari (2008) validated the method proposed by Szalai and Papp (2013) by examining a simply supported steel beam subjected to LTB. However, currently there exists no systematic probabilistic assessment of steel beam sections subjected to LTB. This paper aims to develop a resistance model for LTB valid for a broad range of moment distributions as well as the effect of load height, and to estimate the reliability of these cases if designed per AISC 360 provisions. .

Load Models

During its design lifetime, a structure is subjected to various loads such as dead load, occupancy and roof live loads, wind, snow, and earthquake loads, as well as others. Many interior beams in common braced frame steel construction are not subjected to significant lateral and environmental loads, and hence the load combination that frequently dominates is that of dead load and live load only, which is considered in this study. Dead load (*DL*) statistical parameters are given by Nowak and Szerszen (2003), where *DL* is described as normally distributed with bias factor (ratio of mean value to nominal value) of $\lambda=1.5$ and coefficient of variation (COV) of 0.10.

Occupancy live load represents the weight of people, furniture, partitions and other movable contents, and may be categorized into sustained ("arbitrary-point-in-

time") and transient (extreme event) components. Transient live load considers unusual occurrences of high load concentration such as a large number of people crowding together in a small room. It governs over the sustained effect with the load combination considered in this study, where 50 year maximum load statistics are given by Nowak and Szerszen (2003) as $\lambda=1.0$ and $COV=0.18$. It is assumed to follow a Gumbel distribution (Nowak and Szerszen 2003). In this study, a dead load to total load ratio ($\frac{DL}{DL+LL}$) of 0.2 was selected in order to have the target reliability index in the range of 3.0 to 3.5.

Resistance Model

The failure mode employed in this study is elastic lateral torsional bucking (LTB), where the effect on LTB resistance from different loading patterns and vertical load positions with respect to the shear center is considered. To determine buckling resistance, the elastic stiffness is described using Euler-Bernoulli elastic flexure theory for simply supported beams. The end conditions are taken as warping free and torsionally fixed. The lateral torsional behavior of the beam under these constraint conditions can be described as:

$$\frac{d^4\phi}{dz^4} - \frac{GJ}{EC_w}\frac{d^2\phi}{dz^2} + \frac{y_v v_y(z)}{EC_w}\frac{d\phi}{dz} - \frac{m_x^2(z)}{E^2 I_y C_w}\phi \qquad (103)$$

In Eq. 103, load height is represented as variable component y_v, while angle of twist is given by ϕ. The applied moments and shears are represented as functions $m_x(z)$ and $v_y(z)$, respectively. In this study, these applied moments and shears correspond to the three load distributions considered in Figure 13. In Figure 13, w is the applied load,

z is the variable component in the length direction of the beam (also appearing in Eq. 103), n is the linearity factor, m is the applied end moment, and κ is the end moment factor. By adjusting these factors, various common load types may be recovered from this general distribution including a uniformly distributed load with possible end moments and a linearly increasing distribution load with possible end moments. The applied end moments can be scaled based on the factor κ, and more complex parabolic load distributions can be considered by adjusting the linearity factor n.

Once a desired load distribution is chosen for consideration, the corresponding shear and moment functions are developed. For example, the resulting moment and shear functions for the Type 1 (linearly increasing) distribution shown in Figure 13 are:

$$m_x(z) = -\frac{wz^{n+2}}{(n+1)(n+2)L^n} + \left[\kappa\frac{wL}{(n+2)(n+4)} + \frac{wL}{(n+1)(n+2)}\right]z \tag{104}$$

$$v_y(z) = -\frac{wz^{n+1}}{(n+1)L^n} + \kappa\frac{wL}{(n+2)(n+4)} + \frac{wL}{(n+1)(n+2)} \tag{105}$$

The smallest load value (w) to cause the stiffness of the beam to approach zero is the critical lateral torsional buckling load. This load is converted into a critical moment, M_{cr} and normalized using an equivalent uniform moment factor (EUMF) approach, as given by eq. (106).

$$EUMF = \frac{M_{cr}}{M_{0\_cr}} \tag{106}$$

The EUMF is the ratio of the applied moment needed to cause LTB instability (i.e. the critical load) for the load distribution and boundary conditions considered and

the basic strength. The basic strength, M_{0_cr} is the LTB resistance of a simply supported member subject to a constant moment distribution. The basic strength is taken as (Timoshenko and Gere 1961, Trahair 1998):

$$M_{0\_cr} = \frac{\pi}{L}\sqrt{EI_y GJ\left(1+\frac{EC_w}{GJ}\frac{\pi^2}{L^2}\right)} \tag{107}$$

The EUMF is multiplied by the basic strength of the specific member under consideration to determine its elastic LTB resistance without the need for a complex numerical or finite element analysis. Equivalent uniform moment factor approaches are considered by various design codes. For example, the American Institute of Steel Construction's Specification for Structural Steel Buildings, AISC 360 (AISC 2010) and the American Association of State Highway and Transportation Officials Load and Resistance Factor Design Bridge Design Specifications (AASHTO 2010) use the same expression, and is similar to that proposed by Kirby and Nethercot (1979):

$$C_b = \frac{12.5M_{max}}{2.5M_{max} + 3M_a + 4M_b + 3M_c} \tag{108}$$

C_b, the moment gradient factor, allows approximate consideration of the effects of arbitrary moment distributions. In the standard code procedure, to determine the nominal resistance for elastic LTB, C_b is multiplied by the basic strength (AISC 360):

$$R_n = C_b M_{0\_cr} \tag{109}$$

Although very useful, the drawback to this expression is that it inaccurately describes resistance under certain load situations. The problem is further exacerbated

in that it does not account for vertical load position with respect to the shear center. Because of these drawbacks, rather than basing resistance on Eq.'s 108 and 109, Eq. 103 is set to zero and a finite difference analysis is used to solve for the minimum load *w*, the exact critical load for the load type considered (Types 1 through 3 in Figure 13). For reliability analysis, the nominal elastic LTB resistance is assumed to have a bias factor, λ=*1.03* and COV of 0.12, (Nowak and Collins 2003). Mean resistance is thus taken as $Mcr = \lambda M_{cr}$. In this study, a W14 X 132 simply supported A992 Grade 50 beam with a span of 30 feet is considered to support load distributions Types 1 through 3, combined with three different linearity factors n=0, 1, and 2. The resulting EUMFs are shown in Figures 30-33. The beam is assumed to be subjected to dead and live load with a resulting load combination of 1.2*DL* + 1.6*LL* and designed according to AISC 360 (2010), with strength reduction factor taken as $\phi = 0.9$.

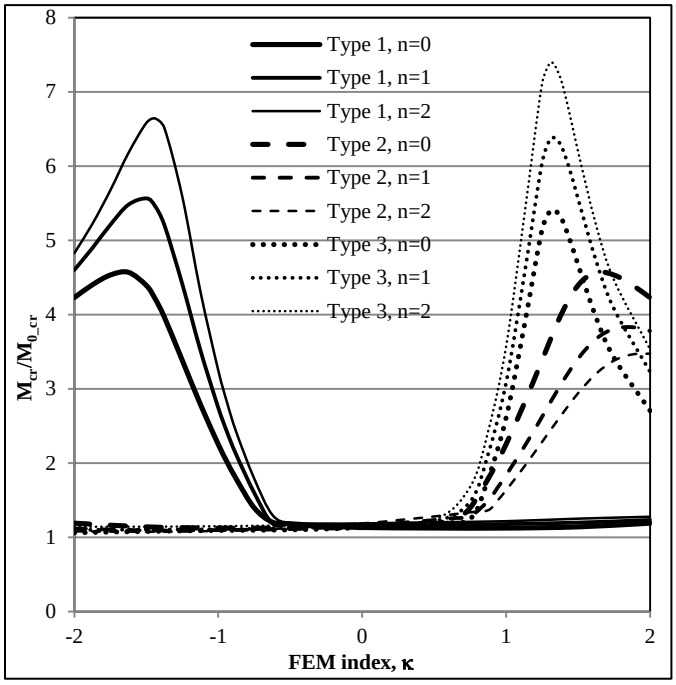

Figure 30: Load Types 1-3 solution for reliability analysis plot, Yv=0

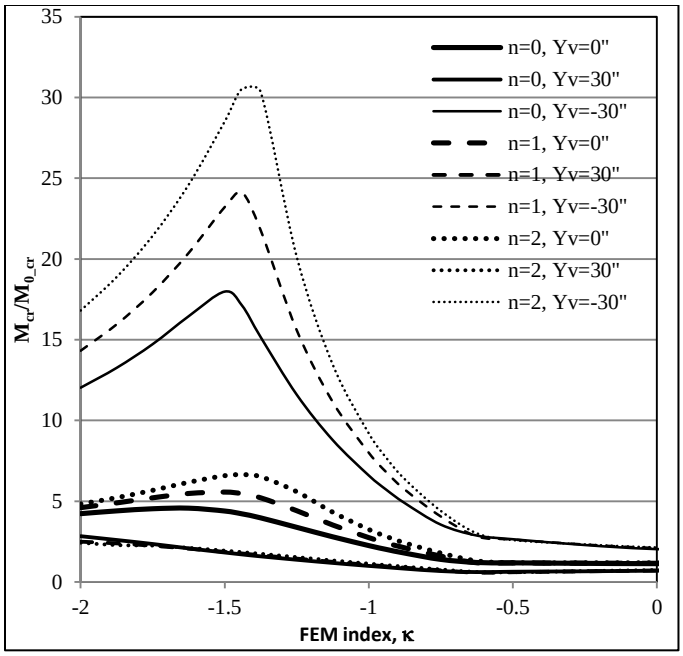

Figure 31: Load Type 1 load height effects, n=0, 1 and 2

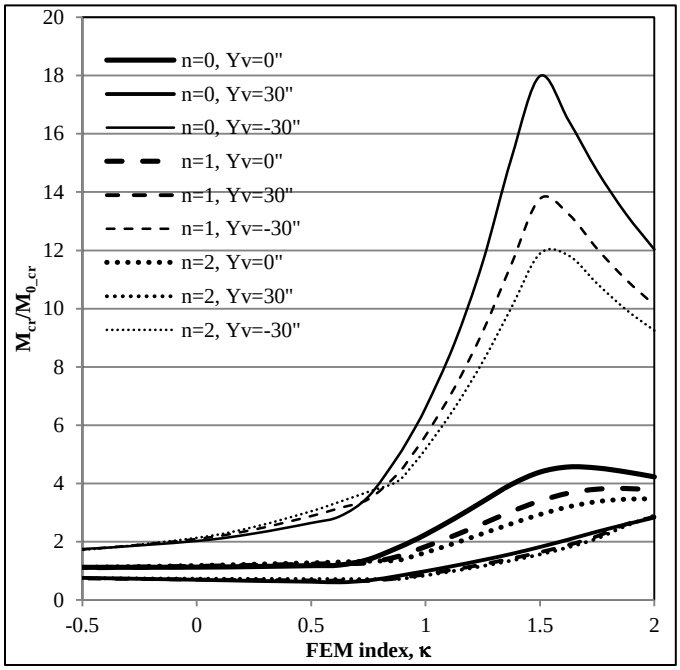

Figure 32: Load Type 2 load height effects, n=0, 1 and 2

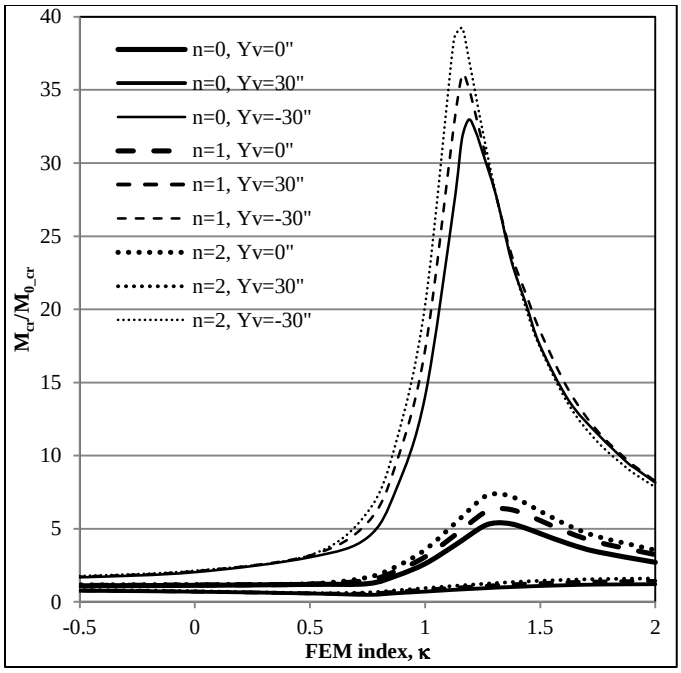

Figure 33: Load Type 3 load height effects, n=0, 1 and 2

Reliability Analysis

Dead load (*DL*), live load (*LL*) and critical LTB moment capacity (*Mcr*) are the random variables (RVs) considered for the analysis, with statistical parameters described above. The resulting limit state function is:

$$g = M_{cr} - DL - LL \tag{110}$$

Monte Carlo Simulation (MCS) is used to compute failure probability p_f, then results are transformed to reliability index with the standard normal transformation $\beta = -\Phi^{-1}(p_f)$.

Results

Results are presented in Figures 34-37, where the reliability index is given as a function of different load types and vertical positions relative to the shear center. Normalizing the critical moments will produce approximately the same results for EUMF for a given load type and for a set of parameters (*E*, *I*, *G* and *J*). This goes to say that the results will be the same for any reasonable stiffness parameters input that allow the member to fail elastically The reliability indices are plotted against the end moment factor index varying from -2 to 2 where an end moment factor of 0 represents a simply supported case with no applied end moments. In Figure 34, where load is applied at the shear center, it can be observed that for all load cases, when the end moment factor κ is between approximately -1 and 1, reliability index falls between 3.0 and 3.5, which is expected, as this is the target reliability range for beams subjected to LTB if designed according to AISC 360 (2010) However, as the load type deviates from uniform, the deviation between the EUMF's obtained from the numerical analysis and that of the AISC 360 approximate method (i.e. as a result of using Eq. 108) increases, reliability index also increases, as Eq. 108 more inaccurately (conservatively) estimates capacity. These cases are those for which the beam experiences reverse curvature bending; i.e. for Type 1 loading, where the end moment factor $\kappa < 0$ and for Type 2 and Type 3 loads, for $\kappa > 0$. It can also be seen that for a Type 1 load, the reliability indices from AISC 360 are fairly consistent for $\kappa > -0.5$, indicating a close match between the code estimation method and the true section capacity. However for $\kappa < -0.5$, significant deviations occur, resulting in much higher reliabilities due to significant overdesign. Similar observations are made for Types 2 and 3 loads where $\kappa > 0.5$, where cases of

reverse curvature bending cause inconsistent, higher levels of reliability. Figures 35, 36 and 37 show the effect of load height. It is observed that when the load is applied below the shear center of the section, the LTB resistance of the member increases due to increased rotational stability and hence reliability index increases. However, since the moment factor guidelines in AISC 360 does not have a provision that adjusts for the effect of load height, the nominal resistance calculated using the code procedure does not change. In these cases, the AISC 360 procedure underestimated beam capacity by as much as 43% for a Type 3 load with linearity factor $n = 2$. This resulted in reliability indices as that are significantly over the target value. Conversely, when the load was applied above the shear center, beam instability increases and, reliability may decrease very significantly. For example, for a Type 1 load with corresponding FEM indices between -0.5 to -1.125, the discrepancy between the moment factors from numerical analysis to those obtained from the AISC 360 procedure reached as high as 50%, resulting in a decrease in section resistance by approximately the same amount, and a correspondingly large decrease in reliability, to such an extent that in some extreme cases, the reliability index falls below zero (i.e. greater than 50% failure probability). Similar phenomena are observed for Type 2 and 3 load cases, where a negative β is recorded for FEM indices between 0.5 to 1.125 and 0.5 to 1.75 respectively.

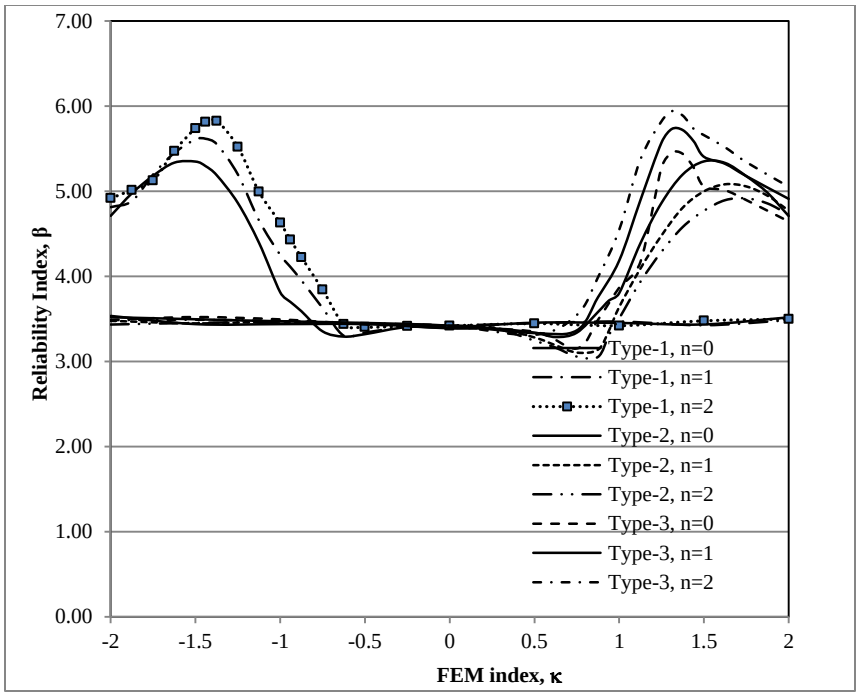

Figure 34: Reliability Indices for Load Types 1-3 with Yv=0

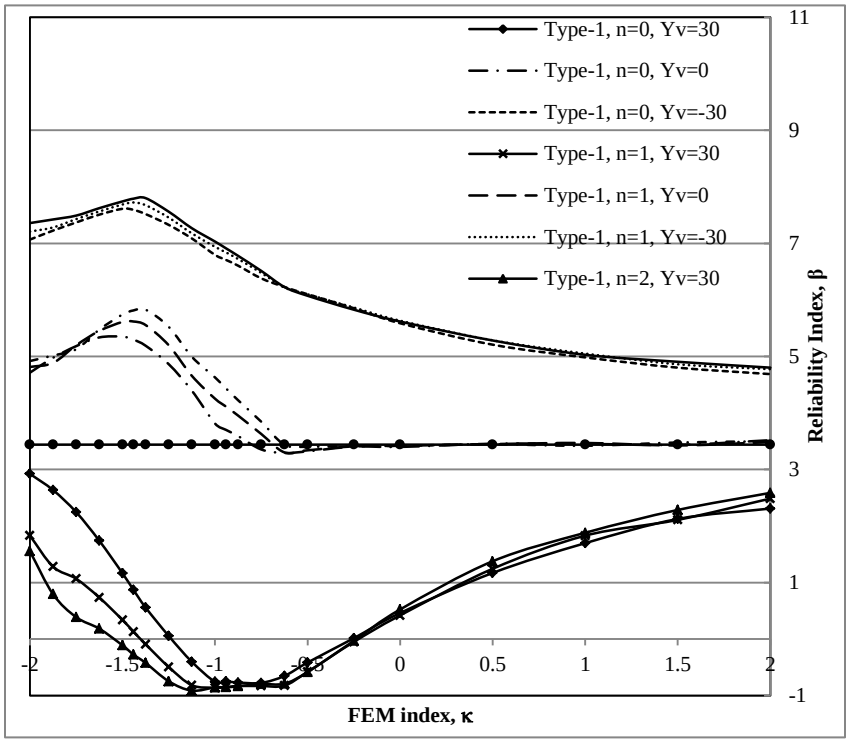

Figure 35: Effect of Load height on Safety Levels for Load Type 1, n=0, 1 and 2

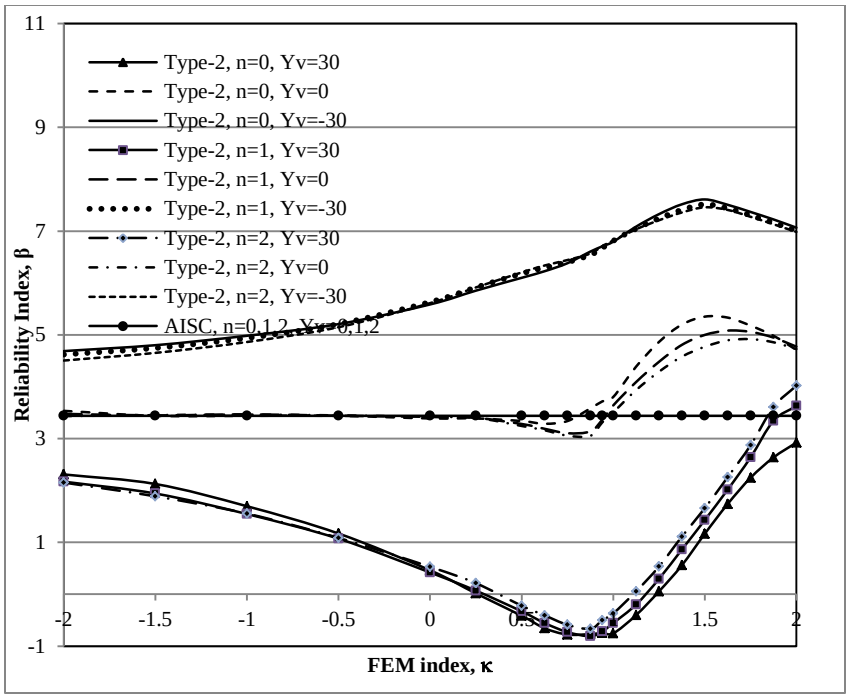

Figure 36: Effect of Load height on Safety Levels for Load Type 2, n=0, 1 and 2

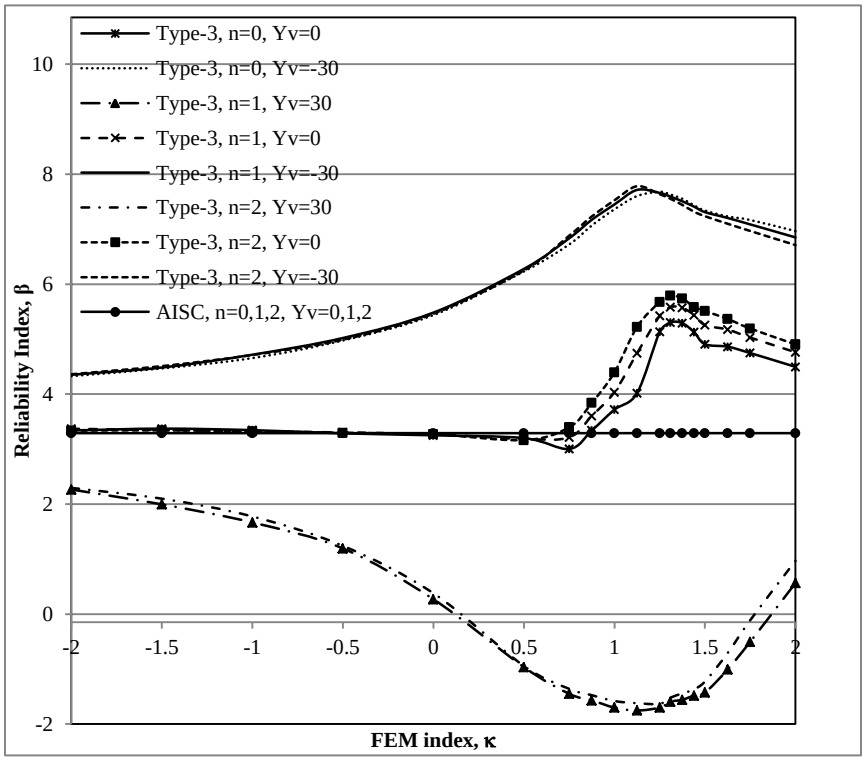

Figure 37: Effect of Load height on Safety Levels for Load Type 3, n=0, 1 and 2

Conclusion

A reliability analysis of the elastic lateral torsional buckling of beams was conducted. The process involves identifying load and resistance random variables, defining the appropriate limit state function, and establishing a suitable resistance model. The resistance model considered in this study properly accounts for the effect of load height under a wide range of moment distributions, where equivalent moment factors were formulated up to 2nd degree spandrel load types. Using this resistance model, it was found that the reliability index of the section investigated experienced a significant change, as a function of load type and position. As expected, the safety level of the beam increased from the target level of approximately 3.5 when load is applied below the shear center, with a reliability index as high as 7.8 for Type 1 loads. Correspondingly, the resistance and thereby the reliability of the beam decreased greatly when load was applied above the shear center, where reliability index was less than zero in some cases. It was also found that when the beam experiences reverse curvature bending, the discrepancy between the AISC 360 procedure to determine LTB capacity and the true solution increased, resulting in increases in reliability index, reflecting the conservativeness of the code procedure in these cases. This occurs for Type 1 distributions when $\kappa < -0.5$, and when $\kappa > 0.5$ for distribution Types 2 & 3.

CHAPTER 8 FINAL CONCLUSION

Introduction

This research involves the study of flexural members as they are subjected to the elastic lateral torsional buckling limit state. To this end, various effects on their stability are discussed with some studied in detail using calculations, figures and design examples. The items studied include moment distribution, load height with respect to the shear center, various types of lateral restraint both discrete and continuous, and the reliability of these members under the effects of moment distribution and load height. Further, a code comparison is done for AISC 360 to understand when circumstances preclude the use of their specifications in designing doubly symmetric wide flange sections for use as flexural members. These areas are selected due to the need that is present in the state of the art and state of the practice in handling the effects described.

Moment Effects

The study of the independent effect of moment distribution between supports has yielded interesting conclusions regarding the current state of the practice in flexural member design. The methods currently ascribed by the prevalent codices around the world prefer approximation methods that are inaccurate under certain design circumstances. These design circumstances found in this study are reflective of a philosophy issue in how flexural member design considering the elastic lateral torsional buckling limit state should be addresses. The current close form approximation method falls short when members are loaded as described in Chapter 3 and in nearly all circumstances where reverse curvature bending is severe. In general this reverse

curvature bending occurs for distribution Type 1 when $\beta < 0$, and for Types 2 and 3 when $\beta > 0$. Unconservative results reach a maximum error from moment effects of 8%. Conservative results reach a maximum error from moment effects of 51%.

Load Height Effects

Load height effects are studied in this paper due to their neglect in prevalent design specifications. This effects absence from design codes is likely due to the difficulty in describing its effect in a general way that is not tailored to specific situations. It is also likely neglected in design codes in part due to the difficulty in factoring in its effects. As shown in Chapter 5, the effects of load height are severe. The strength reduction due to loading members above their shear center is significant with a reduction as high as 75% in some circumstances. Loading members above their shear center can be deceptive as simply applying the loading to the top flange of a wide flange beam effectively loads the beam by a height equal to half the beams depth.

The technical aspects of the study of load height show through intensive derivation that the load height effects are able to be decoupled from those effects associated with moment distribution. In essence this means that a separate factor may be developed for load height that is able to be used in conjunction with existing moment factors and moment factor data. A load height factor is developed and plotted for a series of AISC wide flange steel beams.

Reliability of Flexural Members

A reliability analysis of members subject to elastic lateral torsional buckling is performed using a Monte Carlo Simulation. The analysis is performed considering the effects of moment distribution between supports and load height. A comparison with AISC 360 is used to determine how well these solutions perform in comparison to those specifications mandated by AISC 360. For the independent effect of moment distribution for load types studied, it is shown that as the solution AISC 360 produces deviates from the solution produced by the numerical analysis, the reliability index decreases rapidly. These values occur for all load cases with the end moment factor causes reverse curvature bending as previously described. When the effect of load height is included the reliability index reduces drastically. In most cases the index falls below zero and produces a negative number which indicated a failure rate of 50% or higher. In these circumstances the double effects of reverse curvature bending and load height work together to reduce the ability of AISC 360 in adequately predicting strength member strengths. Separate solution methods for moment effects and load height effects in the form of independent factors are provided to remedy these issues.

Need for Future Research

The need for future research on the topic is mainly described in Chapter 6. The types and levels of lateral-torsional restraint need to be described and studied in further detail. Methods also need to be devised for design codes to use that allow discrete torsional braces to be solved for. Membranes such as fabrics that cover systems of

beams and are assumed to provide bracing also need to be studied. And lastly the restraint that loads provide to members as they load them needs to be studied.

Future work is also needed for load height factors. The curves provided in Chapter 5 for the load height factors that correspond to loading types 1, 2, and 3 only apply to these load types. All of the load types presented in Table 1 need to be studied and described so that all of the most typical design scenarios are covered. Since these factors are developed for double symmetric flexural members, members that are not symmetric such as C and Z shapes need to be studied and have an additional eccentricity applied.

REFERENCES

AASHTO (2012). “AASHTO LRFD Bridge Design Specifications,” American Association of State Highway and Transportation Officials.

AISC 360-10 (2010). “Specification/Commentary for Structural Steel Buildings,” American Institute of Steel Construction.

Austin, Yegian, and Tung (1955). “Lateral Buckling of Elastically End-Restrained I-Beams,” Proceedings of the American Society of Civil Engineers, Vol. 81, p673-1 – 673-25.

Austin (1961). “Strength and Design of Metal Beam-Columns,” Journal of the Structural Division ASCE, Vol. 87, p1-32.

Badari (2013). “Probabilistic Evaluation of Lateral-Torsional Buckling Resistance of Steel Beams.” Second Conference of Junior Researchers in Civil Engineering, p31-40.

BSI (2000). “Structural Use of Steelwork in Building: Code of Practice for Design, Rolled and Welded Sections.” BS5950-1, British Standards Institution.

Clark and Jombock (1957). “Lateral Buckling of I-beams Subjected to Unequal End Moments,” Paper No. 1291, Journal of the Engineering Mechanics Division, ASCE, Vol. 83.

Clark, and Hill (1960). “Lateral Buckling of Beams,” Journal of the Structural Division ASCE, Vol. 86, p175-196.

CSA (2001). “Limit States Design of Steel Structures.” CSA-S16-01, Canadian Standards Association.

CSA (2006). “Canadian Highway Bridge Design Code.”, CSA-S6-06, Canadian Standards Association.

Dumont (1937). “The Lateral Stability of Deep Rectangular Beams,” Technical Note 601, NACA.

Dumont, and Hill (1940). “Lateral Stability of Equal Flanged Aluminum Alloy I-Beams Subject to Pure Bending,” Technical Note 770, NACA.

Eamon and Jensen (2013). “Reliability Analysis of RC Beams Exposed to Fire,” Journal of Structural Engineering, Vol. 139, p212-220.

ECS (1992). “Eurocode 3: Design of Steel Structures.” EN-1993-1-1, European Committee for Standardization.

Flint (1950). “The Stability and Strength of Slender Beams.” Engineering, Vol. 170, p545.

Hibbeler (2009). “Structural Analysis Seventh Edition.” Pearsons Prentice Hall

Hill (1954). “Lateral Buckling of Channels and Z-Beams.” Transactions of the ASCE, Vol. 119, p829.

Kirby, and Nethercot (1979). “Design for Structural Stability,” Halsted Press.

Lopez, Yong, and Serna (2006). “Lateral-Torsional Buckling of Steel Beams: A General Expression for the Moment Gradient Factor,” International Colloquium on Stability and Ductility of Steel Structures, Lisbon, Portugal, 6-8 September, 2006.

Nagle, Saff, and Snider (2004). “Fundamentals of Differential Equations 6th edition,” Pearson Education.

Nethercot, and Rockey (1972). “A Unified Approach to the Elastic Lateral Buckling of Beams,” Engineering Journal, American Institute of Steel Construction, July, pp. 96–107.

Nethercot, and Trahair (1976). “Lateral Buckling Approximations for Elastic Beams,” The Structural Engineer, Vol. 54, p197-204.

Nowak and Collins (2000). “Reliability of Structures.” McGraw-Hill Higher Education.

Nowak and Szerszen (2003). “Calibration of Design Code for Buildings (ACI 318): Part 2 – Reliability Analysis and Resistance Factors.” ACI Structural Journal, Vol. 100, p383-391.

Rebelo, Lopes, Silva, Nethercot and Real (2009). “Statistical Evaluation of the Lateral-torsional Buckling Resistance of Steel I-beams, Part 1- Variability of the Eurocode 3 Resistance Model,” Journal of Constructional Steel Research, Vol. 65, p818-831.

SAA (1998). “Australian Standard – Steel Structures.” AS4100, Standards Australia.

Salvadori (1955). “Lateral Bucking of I-Beams,” ASCE Transactions, Vol. 120, p1165-1177.

Segui (2007). “Steel Design.” CENGAGE Learning.

Serna, Lopez, Puente, and Yong (2006). “Equivalent Uniform Moment Factors for Lateral Torsional Buckling of Steel Members,” Journal of Constructional Steel Research, Vol. 62, p566-580.

Suryoatmono, and Ho (2002). “The Moment Gradient Factor in Lateral-Torsional Buckling on Wide Flange Steel Sections,” Journal of Constructional Steel Research, Vol. 58, p1247-1264.

Szalai and Papp (2009). “On the Probabilistic Evaluation of the Stability Resistance of Steel Columns and Beams,” Journal of Constructional Steel Research, Vol. 65, p569-577.

Trahair (1993). “Flexural-Torsional Buckling of Structures,” Chapman and Hall.

Timoshenko, and Gere (1961). “Theory of Elastic Stability,” McGraw Hill.

Wang, Yuan, Shi, and Cheng (2012). “Lateral-Torsional Buckling Resistance of Aluminum I-Beams,” Thin Walled Structures, Vol. 50, p24.

White, and Kim (2008). “Unified Flexural Resistance Equations for Stability Design of Steel I-Section Members: Moment Gradient Tests,” Journal of Structural Engineering ASCE, Vol. 134, p1471-1486.

Wong, and Driver (2010). “Critical Evaluation of Equivalent Moment Factor Procedures for Laterally Unsupported Beams,” Engineering Journal, American Institute of Steel Construction.

Zuraski (1992). “The Significance and Application of C_b in Beam Design.” Engineering Journal AISC, Vol. 39, p20-25.

ABSTRACT

ELASTIC STABILITY OF FLEXURAL MEMBERS IN CIVIL ENGINEERING DESIGN

by

ALEXANDER W. LAMB

December 2014

Advisor: Dr. Christopher D. Eamon

Major: Civil and Environmental Engineering

Degree: Doctor of Philosophy

The elastic lateral torsional stability of flexural members is studied. The effects of moment distribution between supports and load height with respect to shear center are examined using numerical and analytical methods. From these methods, independent moment and shear factors are developed for a range of load types and load heights. A code comparison is performed comparing numeric results with those produced by AISC 360 to illustrate situations where issues occur in terms of strength prediction. A reliability analysis is performed from this data to quantify the difference in terms of the reliability index using a Monte Carlo Simulation. The results of the analysis show large discrepancies between the results produced by the code and those produced by the numerical analysis in circumstance where reverse curvature bending is apparent. Further, large discrepancies result when the load is positioned above the shear center of the member. This difference indicates a need for the code to change to have special provisions that handle the circumstances surrounding the load types studied and the load height effect. A method is proposed to adjust for these effects by the introduction of

independent moment and load height factors with a design example to illustrate the method.

AUTOBIOGRAPHICAL STATEMENT

I am a 3rd generation civil engineer with ties to Wayne State University and the Civil Engineering Department as my father John Lamb III attended as an engineering student and my grandfather Dr. John Lamb held the position of Department Chairmen. My father obtained a bachelor's degree in Civil Engineering and went on to pursue a career as a geotechnical and hydrological engineer. He spent much of his time in my childhood taking me on job sites and including me in the projects he would occasionally bring home. One project we worked on that stands out in my memory was the bridge competition at Keller Middle School. In working with me on this competition my father taught me the basics of structural mechanics and how to use analysis to solve simple problems. This was very inspirational for me and had a major impact on my decision to pursue structural engineering. We beat the previously held record by something like 4 times the previous weight. In fact the bridge was so robust that the loading apparatus failed causing a particularly dangerous situation for those sitting close by.

My grandfather was quite a significant man. He studied structural engineering and geotechnical engineering at the University of Illinois at Champagne Urbana. He received his master's degree under Nathan Newmark, and was 1 of 13 Ph.D. candidates to receive his degree under Ralph Peck. His master's degree was in structural mechanics and his Ph.D. was in geotechnical engineering. He famously worked for NASA on their Nuclear Ground Shock problem intended to counter the cold war threat of subterranean nuclear missile blasts and also consulted on their Moon Lab project. He spent a term as the manager of the Air Force Office of Scientific Research and Development among other appointments at prestigious institutions.